

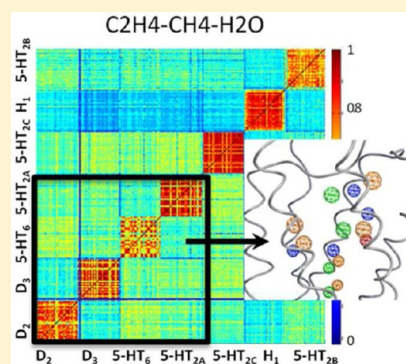
# Addressing Selective Polypharmacology of Antipsychotic Drugs Targeting the Bioaminergic Receptors through Receptor Dynamic Conformational Ensembles

Balaji Selvam, Simon L. Porter, and Irina G. Tikhonova\*

Molecular Therapeutics, School of Pharmacy, Medical Biology Centre, 97 Lisburn Road, Queen's University Belfast, BT9 7BL, Northern Ireland, United Kingdom

## S Supporting Information

**ABSTRACT:** Selective polypharmacology, where a drug acts on multiple rather than a single molecular target involved in a disease, emerges to develop a structure-based system biology approach to design drugs selectively targeting a disease-active protein network. We focus on the bioaminergic receptors that belong to the group of G-protein-coupled receptors (GPCRs) and represent targets for therapeutic agents against schizophrenia and depression. Among them, it has been shown that the serotonin (5-HT<sub>2A</sub> and 5-HT<sub>6</sub>) and dopamine (D<sub>2</sub> and D<sub>3</sub>) receptors induce a cognition-enhancing effect (group 1), while the histamine (H<sub>1</sub>) and serotonin (5-HT<sub>2C</sub>) receptors lead to metabolic side effects and the 5-HT<sub>2B</sub> serotonin receptor causes pulmonary hypertension (group 2). Thus, the problem arises to develop an approach that allows identifying drugs targeting only the disease-active receptors, i.e. group 1. The recent release of several crystal structures of the bioaminergic receptors, involving the D<sub>3</sub> and H<sub>1</sub> receptors, provides the possibility to model the structures of all receptors and initiate a study of the structural and dynamic context of selective polypharmacology. In this work, we use molecular dynamics simulations to generate a conformational space of the receptors and subsequently characterize its binding properties applying molecular probe mapping. All-against-all comparison of the generated probe maps of the selected diverse conformations of all receptors with the Tanimoto similarity coefficient (Tc) enable the separation of the receptors of group 1 from group 2. The pharmacophore built based on the Tc-selected receptor conformations, using the multiple probe maps discovers structural features that can be used to design molecules selective toward the receptors of group 1. The importance of several predicted residues to ligand selectivity is supported by the available mutagenesis and ligand structure–activity relationship studies. In addition, the Tc-selected conformations of the receptors for group 1 show good performance in isolation of known ligands from a random decoy. Our computational structure-based protocol to tackle selective polypharmacology of antipsychotic drugs could be applied for other diseases involving multiple drug targets, such as oncologic and infectious disorders.



## ■ INTRODUCTION

Recently appreciated selective polypharmacology, in which a drug acts on multiple and not a single molecular target involved in a disease, challenges computer-aided drug discovery to find new strategies for the search of drugs modulating a protein network in the disease.

Thus, it has been shown that clinically effective drugs in neurodegenerative, psychiatric, oncologic, and infectious diseases have a complex pharmacological profile and exhibit pleiotropic actions.<sup>1,2</sup> For example, many antipsychotic drugs provide therapeutic effect by interacting with several bioaminergic G protein-coupled receptors (GPCRs)<sup>3</sup> or kinase inhibitors demonstrate their anticancer effect through their action on multiple signaling kinases.<sup>1</sup> Since the causes of these diseases are not fully understood, the attempts to develop a drug targeting one of the proteins involved in the disease have not been fruitful.<sup>2</sup> The advantages of the multitarget therapy strategies have been also recognized for infectious diseases in order to avoid resistance, improve dose regime and minimize toxicity of the drugs.<sup>4</sup>

A task, however, to find drugs that modulate several disease active members of the same protein family and do not bind to other members is very difficult, especially for GPCRs, kinases and proteases. One of the reasons is that residues forming the drug binding cavity within a protein family are similar, enabling recognition of a drug by many members of a family. On the other hand, similar residues of other members fail to bind the same drug, likely as result of different conformations. Because of that, understanding of selective polypharmacology cannot be gained only through the analysis of sequences or a single three-dimensional structure of a protein family member but must also involve protein flexibility. In this work, we aim to explore protein flexibility within the bioaminergic receptor family using molecular dynamics (MD) simulations to examine the molecular context of selective polypharmacology.

Consideration of protein flexibility in the structure-based drug design against one drug target has been proved to be

Received: May 13, 2013

Published: June 23, 2013

critical in understanding molecular recognition and designing novel binders for enzymes and receptors.<sup>5,6</sup> Thus, multiple protein conformations with identified novel druggable binding regions and binding modes of ligands were important in finding novel inhibitors of HIV-1 integrase,<sup>7</sup> RNA-editing ligase 1,<sup>8</sup> UDP-galactose 4'-epimerase,<sup>9</sup> neuraminidase,<sup>10</sup> and MDM2-p53 interactions.<sup>11</sup> In addition, it has been shown that the protein flexibility is often a mechanism of ligand subtype and subspecies selectivity. In particular, the ligand subtype selectivity in the ionotropic glutamate,<sup>12</sup> estrogen,<sup>13</sup> thyroid hormone,<sup>14</sup> the nicotinic acetylcholine,<sup>15</sup> and  $\beta$  adrenergic receptors<sup>16</sup> was linked with protein conformational diversity in the computational studies. The pharmacophore model for dihydrofolate reductase inhibition derived from multiple crystal structures has indicated subtle differences between human and *Pneumocystis carinii* species of the enzyme and was used to design inhibitors targeting preferably the fungal enzyme and, therefore, preventing side effects.<sup>17</sup> The protein flexibility derived from MD simulations was used in identification of the molecules that have a distinct inhibition profile across the species of thymidylate synthase.<sup>18</sup>

Structural flexibility has been probed in understanding of selective polypharmacology in one study in the literature.<sup>19</sup> Thus, MD simulations of selected kinases were used to probe the selective polypharmacology of nelfinavir, an HIV-protease inhibitor, to multiple kinases in order to explore the anticancer activity of nelfinavir.<sup>19</sup> The results of the computational study were in agreement with kinase activity assays and available clinical studies.

To further examine the importance of structural flexibility in selective polypharmacology, we focus on the bioaminergic receptors, which are the targets for therapeutic agents against schizophrenia and depression. Among them, it has been shown that a number of the serotonin (5-HT<sub>2A</sub> and 5-HT<sub>6</sub>) and dopamine (D<sub>2</sub> and D<sub>3</sub>) receptors induce a cognition-enhancing effect (group 1), while the histamine (H<sub>1</sub>) and serotonin (5-HT<sub>2C</sub>) receptors lead to metabolic side effects and the serotonin (5-HT<sub>2B</sub>) receptor causes pulmonary hypertension (group 2).<sup>2</sup> Thus, the task is to develop an approach that enables to find drugs targeting preferably the disease-active receptors, i.e. group 1.

The recent release of several crystal structures of the bioaminergic receptors, including the D<sub>3</sub> and H<sub>1</sub> receptors<sup>20,21</sup> has provided the possibility to model the structures of these receptors and study the molecular context of selective polypharmacology for the first time. Thus, the structural snapshot of the receptors allows initiating the study of the receptor dynamic nature. We hypothesize that accounting for receptor flexibility within this receptor family might help understand differences between the groups of the receptors.

In this work, we present a computational structure-based protocol that can be used to rationalize selective polypharmacology of antipsychotic drugs. Beginning with 3D models of the seven bioaminergic receptors (5-HT<sub>2A</sub><sup>1</sup> (group allocation is in the superscript here and throughout the manuscript), 5-HT<sub>6</sub><sup>1</sup>, D<sub>2</sub><sup>1</sup>, D<sub>3</sub><sup>1</sup>, H<sub>1</sub><sup>2</sup>, 5-HT<sub>2C</sub><sup>2</sup>, and 5-HT<sub>2B</sub><sup>2</sup>) and characterization of their physicochemical and geometrical properties, conventional molecular dynamics simulations of the receptors are performed in order to investigate flexibility of ligand binding cavities. We then propose all-against-all comparison of the generated receptor conformational spaces of the bioaminergic receptors via unifying their binding properties with a help of molecular probe mapping. The multiple probe maps of the receptor

conformations are then analyzed with the volume-based Tanimoto similarity coefficient<sup>22</sup> and used to derive pharmacophoric sites for the receptors of group 1. Finally, the selected receptor conformations were tested in the retrospective screening. Our study provides a structural and dynamic basis of selective polypharmacology of antipsychotic drugs targeting the bioaminergic receptors.

## METHODS

**Preparation of the Bioaminergic Receptors.** The amino acid sequences of the D<sub>2</sub>, 5-HT<sub>2A</sub>, 5-HT<sub>2B</sub>, 5-HT<sub>2C</sub>, 5-HT<sub>6</sub>, and H<sub>1</sub> receptors are obtained from the Expasy web server. The sequence alignment was adjusted manually to match the known conserved motifs of the helices (Figure 1S of the Supporting Information). The homology models of the D<sub>2</sub>, 5-HT<sub>2A</sub>, 5-HT<sub>2B</sub>, 5-HT<sub>2C</sub>, and 5-HT<sub>6</sub> receptors are built based on the D<sub>3</sub> crystal structure<sup>20</sup> as a template with the PDB code: 3PBL using the Prime module 3.0 of the Schrodinger suite 2011.<sup>23,24</sup> In the published crystal structure of the H<sub>1</sub> receptor (PDB code: 3RZE),<sup>21</sup> the six residues (168–174) of the second extracellular loop are not crystallized and have been remodelled using the Prime module. All final models were energy minimized using the CHARMM force field.<sup>25</sup> The geometry of the built homology models was further validated using PROCHECK.<sup>26</sup>

**Molecular Dynamics (MD) Simulations.** All simulations were performed using the Desmond program, version 2.2.<sup>27</sup> The biosystem involving the receptor and water–lipid environment was built using System Builder in Maestro GUI, version 9.2,<sup>24</sup> and neutralized by adding contra-charged ions. The system was equilibrated before starting the production phase of the MD simulations. Before equilibration, the solvent molecules and the lipid bilayer were minimized using the conjugate gradient and steepest descent algorithms up to a convergence of 0.5 kcal/(mol Å). The system was slowly heated with constant volume and equilibrated for 5–7 ns at 300 K with constant pressure to conduct production runs. The temperature and pressure were controlled at 300 K and 1 atm, respectively, by the Berendsen algorithm. Long-range electrostatics was calculated by means of the Particle Mesh Ewald Method.<sup>28</sup> The production phase has been conducted for 50 ns three times for each receptor using different starting velocities.

**Receptor Conformational Space Analysis.** The rmsd, rmsf, sasa, and the number of water molecules in the ligand binding cavity are calculated using VMD1.9.1.<sup>29</sup> The volume of the binding cavity was calculated using the POVME script,<sup>30</sup> the selected residues for the volume calculation are summarized in Table 1S of the Supporting Information. The default cutoff of 2.5 Å is used for hydrogen bonds. The MD trajectories were clustered using g\_cluster of the Gromacs program.<sup>31</sup> The 0.13 and 0.16 Å cutoff is used for clustering of the trajectories and the obtained clusters were visualized using the clustering plugin-third party tool of VMD1.9.1.

The multifragment search module of the MOE2011.10 program<sup>32</sup> was used for placing of molecular probes into the binding cavity and the obtained probe poses were energy minimized using MMFF94. We used H<sub>2</sub>O, CH<sub>4</sub>, C<sub>2</sub>H<sub>4</sub>, CH<sub>2</sub>O, NH<sub>4</sub>, and dummy atoms as molecular probes.

The ROCS 3.1.2 and EON 2.1.0 programs from the OpenEye software<sup>22</sup> were used for shape and electrostatics matching of the probe maps using the Tanimoto coefficient. The shape comparison is conducted by comparison volume overlay or volume mismatch of the probe map. Thus, the

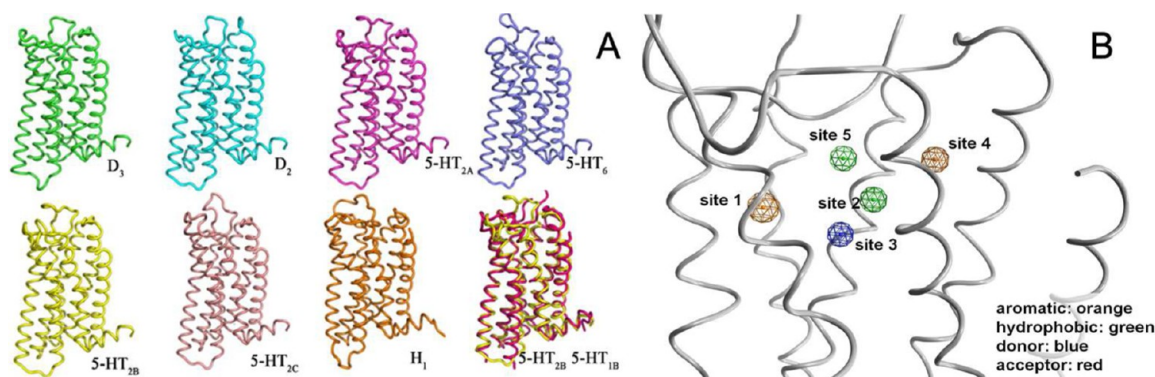


**Figure 1.** Common architecture and pharmacophoric sites of the bioaminergic receptors. (A) Crystal structures of the D<sub>3</sub> and H<sub>1</sub> receptors and the homology models of the D<sub>2</sub>, 5-HT<sub>2A</sub>, 5-HT<sub>6</sub>, 5-HT<sub>2B</sub>, and 5-HT<sub>2C</sub> receptors used in the MD simulations study. The superimposition of the homology model of 5-HT<sub>2B</sub> (yellow) with the recently published crystal structure of 5-HT<sub>1B</sub> (purple) is shown. (B) Pharmacophoric sites from the crystal structures and homology models of the receptors used as initial structures for MD simulations. Pharmacophoric sites were identified from molecular probe mapping.

difference in the volume ( $V$ ) of the two probe maps,  $A_{(x1, y1, z1)}$  and  $B_{(x2, y2, z2)}$  are defined as

$$V = \int |A_{(x1, y1, z1)} - B_{(x2, y2, z2)}| dv$$

where  $x1, y1, z1$  and  $x2, y2, z2$  are the coordinates of the probe maps  $A$  and  $B$  and  $dv$  is the integral of the coordinates of the probe maps.

When the probe maps  $A$  and  $B$  have the identical volume, the difference between the maps is zero and hence the integral is zero. The difference and integral will be large when both probe maps have an entirely different shape. On the basis of the triangle inequality, the distance between the two maps are written as

$$V^2 = \sqrt{\int [A_{(x1, y1, z1)} - B_{(x2, y2, z2)}]^2 dv}$$

and the equation can be rewritten as

$$V^2 = \int [A_{(x1, y1, z1)}]^2 dv + \int [B_{(x2, y2, z2)}]^2 dv - 2 \int A_{(x1, y1, z1)} B_{(x2, y2, z2)} dv$$

The first two terms represent the independent orientation of the maps  $A$  and  $B$ , and the last term is the overlap between the maps  $A$  and  $B$ . To find the best overlay between the objects the similarity measurement called as a Tanimoto coefficient ( $Tc$ ) is calculated by combining the maps  $A$  and  $B$ :

$$Tc = \frac{OA_{(x1, y1, z1)} B_{(x2, y2, z2)}}{A_{(x1, y1, z1)} + B_{(x2, y2, z2)} - OA_{(x1, y1, z1)} B_{(x2, y2, z2)}}$$

where  $OA_{(x1, y1, z1)} B_{(x2, y2, z2)}$  is the overlap between the maps  $A$  and  $B$ .

The Tanimoto value is 1 when the object has the identical shape and varies based on the degree of overlap between the objects.

Once the ROCS shape similarity is calculated, we compare the electrostatic potential of the prealigned probe maps using EON.<sup>22</sup> The results were analyzed with the Vida 4.2.1 module of OpenEye<sup>22</sup> and using the in-house scripts. The matrix plots were generated with MatLab R2009a.<sup>33</sup> The pharmacophore module of MOE2011.10<sup>32</sup> was used for generating the common pharmacophore sites from the probe maps.

**Retrospective Screening.** The structures were refined and prepared using the Protein preparation module of the Maestro 9.2. The binding site residues used in the binding cavity analysis were selected for the docking grid generation. The available ligands for the seven investigated receptors with the preference toward the receptors of group 1 and the ligands selective for one receptor of group 1 were collected from the literature sources (Table S3 of the Supporting Information). This library was merged with 500 randomly selected diverse compounds from the Maybridge database 2012. All compounds were prepared using the LigPrep module 2.5 of the Schrodinger suite 2011.<sup>24</sup> All docking runs were performed using the SP scoring function of Glide 5.7.<sup>34</sup> The compounds interacting with Asp at position 3.32 were considered docked correctly and used to calculate the enrichment factor. The docking poses of the known ligands have been verified with other modeling studies, available residue mutagenesis and structure–activity relationships of ligands.<sup>35–37</sup>

## RESULTS

**Structural Models of the Bioaminergic Receptors.** We have used the crystal structures of the H<sub>1</sub> and D<sub>3</sub> receptors<sup>20,21</sup> and the homology modes of the D<sub>2</sub>, 5-HT<sub>6</sub>, 5-HT<sub>2A</sub>, 5-HT<sub>2B</sub>, and 5-HT<sub>2C</sub> receptors (Figure 1A) constructed based on the D<sub>3</sub> crystal structure in this study. The sequence similarity of transmembrane regions and extracellular loops between the D<sub>3</sub> receptor and other bioaminergic receptors is over 35%, which is sufficient to build reliable models of the receptors.<sup>38</sup> Interestingly, the crystal structure of 5-HT<sub>1B</sub> with resolution 2.8 Å has been released when the manuscript was in preparation, which has over 85% sequence similarity with 5-HT<sub>2B</sub> (PDB code: 4IAQ<sup>39</sup>). We found that the Cα root mean-square deviation (rmsd) between our model and the crystal structure is 1.5 Å, supporting the reliability of the 5-HT<sub>2B</sub> homology model (Figure 1A).

To start a comparison of the orthosteric ligand binding sites of the bioaminergic receptors, we have calculated the sequence similarity, volume and hydrophobic and hydrophilic solvent-accessible surface areas (SASA) of the binding cavity as shown in Table S1 of the Supporting Information. It is evident that the binding cavity of all receptors involving the residues within 6 Å from the ligand has high sequence similarity. The binding cavity forming by helices 6 and 7 has 99% similarity, while forming by



Table 1. Summary of Molecular Dynamics Simulations<sup>a</sup>

receptor	sim time, ns	sim runs	$\text{C}\alpha$ rmsd <sub>rec</sub> , Å	$\text{C}\alpha$ rmsf <sub>cav</sub> , Å	$V_{\text{cav}}$ , Å <sup>3</sup>	SASA <sub>b_cav</sub> , Å <sup>2</sup>	SASA <sub>s_cav</sub> , Å <sup>2</sup>	SASA <sub>phi</sub> , Å <sup>2</sup>	SASA <sub>phob</sub> , Å <sup>2</sup>	$N_{\text{wat}}$
D <sub>2</sub>	50	3	1.7 ± 0.2	1.7 ± 0.3	520 ± 15	91 ± 10	519 ± 12	143 ± 5	468 ± 4	27 ± 6
D <sub>3</sub>	50	3	2.0 ± 0.2	1.5 ± 0.2	569 ± 48	63 ± 7	534 ± 48	272 ± 7	290 ± 55	22 ± 4
5-HT <sub>6</sub>	50	3	1.8 ± 0.2	1.4 ± 0.2	310 ± 70	81 ± 11	350 ± 70	161 ± 30	253 ± 20	18 ± 2
5-HT <sub>2A</sub>	50	3	2.2 ± 0.3	1.4 ± 0.4	647 ± 107	90 ± 2	586 ± 30	212 ± 10	498 ± 20	21 ± 4
5-HT <sub>2C</sub>	50	3	2.2 ± 0.3	1.5 ± 0.2	697 ± 71	109 ± 5	628 ± 25	233 ± 23	424 ± 34	22 ± 5
H <sub>1</sub>	50	3	2.1 ± 0.2	1.5 ± 0.3	513 ± 90	68 ± 13	542 ± 15	233 ± 6	375 ± 25	26 ± 3
5-HT <sub>2B</sub>	50	3	2.7 ± 0.2	2.2 ± 0.2	559 ± 99	98 ± 10	528 ± 47	222 ± 21	450 ± 54	20 ± 3

<sup>a</sup> $\text{C}\alpha$  rmsd<sub>rec</sub> is the  $\text{C}\alpha$  rmsd of the receptor,  $\text{C}\alpha$  rmsf<sub>cav</sub> is the  $\text{C}\alpha$  rmsf of the binding cavity,  $V_{\text{cav}}$  is the volume of the binding cavity, SASA<sub>b\_cav</sub> is the solvent accessible surface area of the backbone of the residues forming the binding cavity, SASA<sub>s\_cav</sub> is the SASA of the side chain of the residues forming the binding cavity, SASA<sub>phi</sub> is the SASA of the hydrophilic residues of the binding cavity, SASA<sub>phob</sub> is the SASA of the hydrophobic residues of the binding cavity, and  $N_{\text{wat}}$  is the number of water molecules in the binding cavity.

helices 2, 3, and 5 has 55–78% similarity. The volume of the binding cavity is in the range of 368–624 Å<sup>3</sup> in group 1 and 296–552 Å<sup>3</sup> in group 2 of the receptors. The SASA of the hydrophobic residues is significantly higher compared to the SASA of the hydrophilic residues for the D<sub>2</sub><sup>1</sup>, 5-HT<sub>2A</sub><sup>1</sup>, 5-HT<sub>2C</sub><sup>2</sup>, H<sub>1</sub><sup>2</sup>, and 5-HT<sub>2B</sub><sup>2</sup> receptors, i.e. 416/96, 384/113, 286/125, 173/296, and 351/854 Å<sup>2</sup>, respectively, and to a lesser extent, in the D<sub>3</sub><sup>1</sup> receptor (200/257 Å<sup>2</sup>). In contrast, SASA of the hydrophilic residues is higher than SASA of the hydrophobic residues in the 5-HT<sub>6</sub><sup>1</sup> receptor (279/239 Å<sup>2</sup>).

Volume and SASA provide the overall description of the receptor binding cavity. To identify and compare likely binding regions within the binding cavity of the receptors, we used molecular probe mapping. This involved placing molecular probes, such as CH<sub>4</sub>, C<sub>2</sub>H<sub>4</sub>, or H<sub>2</sub>O, to the binding cavity to measure hydrophobic, aromatic and hydrophilic interactions in the putative binding regions. On the basis of the generated probe maps, we then subsequently identified the pharmacophoric sites that are necessary to form interactions with the receptors.

The pharmacophore site is defined when at least one probe of four of seven receptors is placed at the similar position in the binding cavity with the 1.5 Å distance cutoff. The details of the probe mapping are shown in Table 2S of the Supporting Information and the identified pharmacophoric sites are in Figure 1B. Three pharmacophoric sites 1, 2, and 3, i.e., one aromatic, one hydrophobic, and one donor site are corresponded to the common pharmacophore sites, in which one of the molecular probes is mapped in all receptors with the favorable interaction energy. The property of the pharmacophoric site has been established based on the probe providing the lowest interaction energy (Table 2S). The identified common pharmacophore accounts for the general molecular interaction capacities of ligands toward the bioaminergic receptors. The amino acid residues forming these sites are identical in all receptors (Table 2S). One aromatic and one hydrophobic sites, i.e. 4 and 5 are present in the 5-HT<sub>2A</sub><sup>1</sup>, D<sub>2</sub><sup>1</sup>, and D<sub>3</sub><sup>1</sup> receptors of group 1 and the 5-HT<sub>2B</sub><sup>2</sup> receptor of group 2, providing some differences between the groups of the receptors.

From the comparison of the geometrical and physiochemical properties of the receptor binding cavities and their binding regions using the single receptor structure, it is unfeasible to split the receptors structurally into groups 1 and 2, and therefore, to guide structure-based design of selective ligands toward group 1. We further explore the receptor conformational space using the MD simulations to investigate structural

dynamic features between the receptors aiming to understand the molecular potential of selective polypharmacology.

**Dynamics of the Ligand Binding Cavity in the Bioaminergic Receptors.** We have conducted 50 ns MD simulations of seven unliganded bioaminergic receptors in the water–lipid bilayer. The unliganded form of the receptors was chosen to explore flexibility of the binding cavity of the receptors in order to not bias conformations of the cavity to the particular scaffold and volume, which happens in the presence of a ligand. For the goal of our study, it is critical to sample the most diverse conformational space. The ligand induced-fit effect of the bioaminergic receptors is likely subtle, involving little changes in side chains and backbones, which can be sampled on time scales accessible to MD simulations. Indeed, comparison of the recently resolved crystal structure of the  $\beta_1$  adrenergic receptor in the free form<sup>40</sup> with the crystal structure in the ligand bound state<sup>41</sup> shows little changes in the binding pocket with the 1 Å rmsd of the heavy atoms in the binding site.

To increase the conformational sampling we repeated the simulations for each receptor three times using the random initial velocities. The summary of the simulations is shown in Table 1. The  $\text{C}\alpha$ -rmsd is stable and relatively similar in the receptors, with a slightly higher value for the 5-HT<sub>2B</sub><sup>2</sup> receptor. To explore the conformational dynamics of the ligand binding cavity in each receptor we have calculated the  $\text{C}\alpha$  root mean-square fluctuation (rmsf) of the residues lining the binding cavity, the average volume of the cavity, the SASA of the residue backbones and side chains as well as the SASA of the hydrophilic and hydrophobic residues in the simulated receptors. The average  $\text{C}\alpha$ -rmsf of the binding cavity residues shows that the fluctuation of backbone atoms is small in the receptors with a slightly higher value in the 5-HT<sub>2B</sub><sup>2</sup> and D<sub>2</sub><sup>1</sup> receptors.

The average volume in the simulated structures is higher in all receptors compared to the volume of the initial structures (the crystal structures and homology models), arranging the receptors in the following order: 5-HT<sub>6</sub><sup>1</sup> < D<sub>2</sub><sup>1</sup> < H<sub>1</sub><sup>2</sup> < D<sub>3</sub><sup>1</sup> < 5-HT<sub>2B</sub><sup>2</sup> < 5-HT<sub>2A</sub><sup>1</sup> < 5-HT<sub>2C</sub><sup>2</sup>, where the 5-HT<sub>6</sub><sup>1</sup> receptor has the smallest volume and the 5-HT<sub>2C</sub><sup>2</sup> receptors has the largest volume. In addition, we noted high variation of the volume in simulations of all receptors, with the exception of the D<sub>2</sub><sup>1</sup> receptor.

The comparison of the backbone and side chain SASA values shows the high contribution of the side chains to the dynamics of the cavity. Unlike soluble proteins, which often have high fluctuation of the backbones in the ligand binding cavity, the restriction in the mobility of the backbone in the bioaminergic

receptors is evident as the binding cavity is localized within the receptor helical bundle embedded into the membrane bilayer. We noted the higher variation of the hydrophobic SASA in all receptors compared to the hydrophilic SASA, suggesting likely appearance of novel hydrophobic binding regions in the binding cavity. Thus, the average hydrophobic SASA arranges the receptors as  $5\text{-HT}_6^1 < \text{D}_3^1 < \text{H}_1^2 < 5\text{-HT}_{2\text{C}}^2 < \text{D}_2^1 < 5\text{-HT}_{2\text{B}}^2 < 5\text{-HT}_{2\text{A}}^1$ , where the  $5\text{-HT}_6$  receptor is the least hydrophobic and the  $5\text{-HT}_{2\text{A}}$  receptor is the most hydrophobic receptor.

All binding cavities of the receptors have been hydrated in the simulations. The water molecules filled the cavities at the beginning of the simulations and constantly exchanged with the bulky water from the extracellular side. Overall, the binding cavity of the receptors is relatively equally hydrated with less hydration in the  $5\text{-HT}_6^1$  receptor and greater in the  $\text{D}_2^1$  receptor.

We have conducted further clustering of the receptor binding cavities based on the rmsd of the heavy atoms of the residues lining the cavity using a different rmsd cutoff to explore the structural diversity of the generated receptor conformational space. The graph reflecting the relationship between the number of receptor structure clusters and the chosen rmsd cutoff is shown in Figure 2. On the basis of the obtained

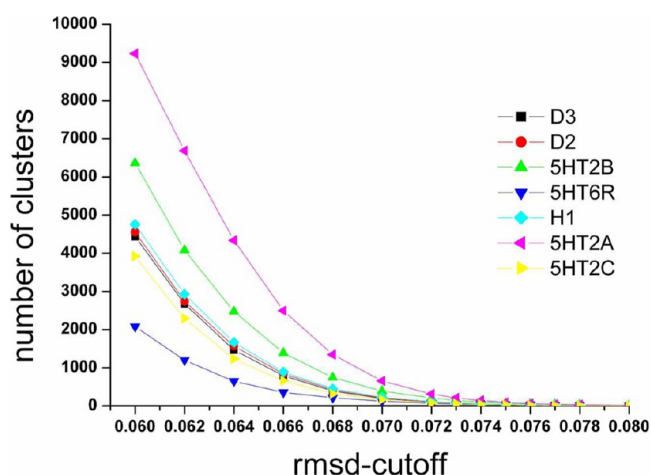


**Figure 2.** Number of clusters versus the rmsd-cutoff (Å) used in clustering of the binding cavity heavy atoms. The clustering procedure was carried out involving three 50 ns simulations for each receptor.

variation of the number of structural clusters, the receptors can be placed in the following order:  $5\text{-HT}_6^1 < 5\text{-HT}_{2\text{C}}^2 < \text{D}_2^1 \approx \text{D}_3^1 < \text{H}_1^2 < 5\text{-HT}_{2\text{B}}^2 < 5\text{-HT}_{2\text{A}}^1$ , where the lowest conformational diversity is in the  $5\text{-HT}_6$  receptor, the highest is in the  $5\text{-HT}_{2\text{A}}$  receptor, and the dopamine receptors  $\text{D}_2^1$  and  $\text{D}_3^1$  have relatively equal conformational diversity.

The analysis of the receptor conformational ensembles indicates significant flexibility and high conformational diversity in the ligand binding cavities, suggesting the occurrence of novel binding regions that might be used for ligand design. We therefore explored the binding capacities of the MD conformations of the bioaminergic receptors employing molecular probe mapping.

**Molecular Probe Mapping of the Receptor Binding Cavity MD Conformations.** To identify the most similar conformations within group 1 of the receptors, which are also the most different from group 2 of the receptors, we have

compared the geometrical and physicochemical properties of the ligand binding cavity in 30 representative conformations of each receptor obtained from three 50 ns trajectories. The selection of conformations has been made to accelerate the next comparison of the receptor binding properties. To identify 30 conformations for a receptor we first have clustered the heavy atoms of the residues, forming the binding cavity in each trajectory using the 0.13 Å cutoff and obtained 100–263 clusters. Next, we merged the representative of the obtained clusters from three trajectories and again clustered the combined conformations using the 0.16 Å cutoff. We expect this strategy in clustering would enable us to select the diverse conformations. The representative of the first 30 populated clusters has been used for the property analysis. For characterization of the hydrophobic and hydrophilic properties of the receptor conformations we have filled the binding cavity with different types of probe molecules ( $\text{CH}_4$ ,  $\text{C}_2\text{H}_4$ ,  $\text{H}_2\text{CO}$ ,  $\text{NH}_4$ , or  $\text{H}_2\text{O}$ ), where they are capable of forming favorable interactions with the residues of the binding cavity. To measure the shape of the binding cavity we use dummy atoms.

The obtained probe map from one probe type in one conformation of a receptor was compared with the same type probe map of other conformations of the receptor using the shape and electrostatic Tanimoto similarity coefficient (Tc) as implemented in the ROCS and EON modules of the OpenEye software.<sup>22,42,43</sup> In ROCS, the shape comparison is conducted by evaluation of volume match or mismatch of the small molecule ligand, binding site or electron density.<sup>22</sup> In our work the query shape is the volume of the probe map. Once the ROCS shape similarity is calculated, the electrostatic potential of the prealigned probe maps is compared using EON.<sup>22</sup> Thus, when Tc is equal to 1 the probe maps are identical and when Tc is equal to 0 the probe maps have no similarity. All-against-all probe map comparison for each type of probe was then conducted for 30 selected conformations of a receptor and between 30 conformations of all receptors. We used the electrostatic Tc to compare the  $\text{H}_2\text{CO}$ ,  $\text{NH}_4$ , and  $\text{H}_2\text{O}$  probes and the shape Tc to compare the  $\text{C}_2\text{H}_4$ ,  $\text{CH}_4$ , and dummy probes. The obtained Tc matrices for each type of the probe are shown in Figure 3.

High variation of Tc values in the Tc matrix plot across 30 conformations of the receptor is observed for several probes, indicating differences in the physicochemical properties and shape of the binding cavity in the receptor conformations. The Tc matrix plot based on the comparison of the dummy atoms, which reflects the shape of the cavity, varies in the range of 0.3–0.6 between the receptors, suggesting low similarity in shape of the binding cavities. The variation of shape Tc values is in correlation with high fluctuation of the binding cavity volume and SASA in the simulations (see above). The Tc matrix built based on the  $\text{NH}_4$  probe has the highest Tc values in all receptors for all conformations, which is likely due to the common feature of having ASP in all receptors that interacts with the quaternary ammonium ion of a ligand. The plot derived from the Tc comparison of  $\text{C}_2\text{H}_4$ , a probe imitating the aromatic property, has the next highest similarity Tc values within and between the groups of the receptors, with a slightly lower value for the  $\text{D}_3$  receptor, which indicates common aromatic features in the receptors. Note, Tc of  $\text{CH}_4$  and  $\text{H}_2\text{O}$  probes has high values for some conformations within group 1 and the  $5\text{-HT}_{2\text{C}}^2$  receptor, suggesting similarity in some hydrophobic and hydrophilic regions in the receptors. The  $\text{H}_2\text{CO}$  map shows high similarity between the  $5\text{-HT}_{2\text{A}}^1$ ,  $5\text{-HT}_{2\text{B}}^2$ , and  $5\text{-HT}_{2\text{C}}^2$  receptors.



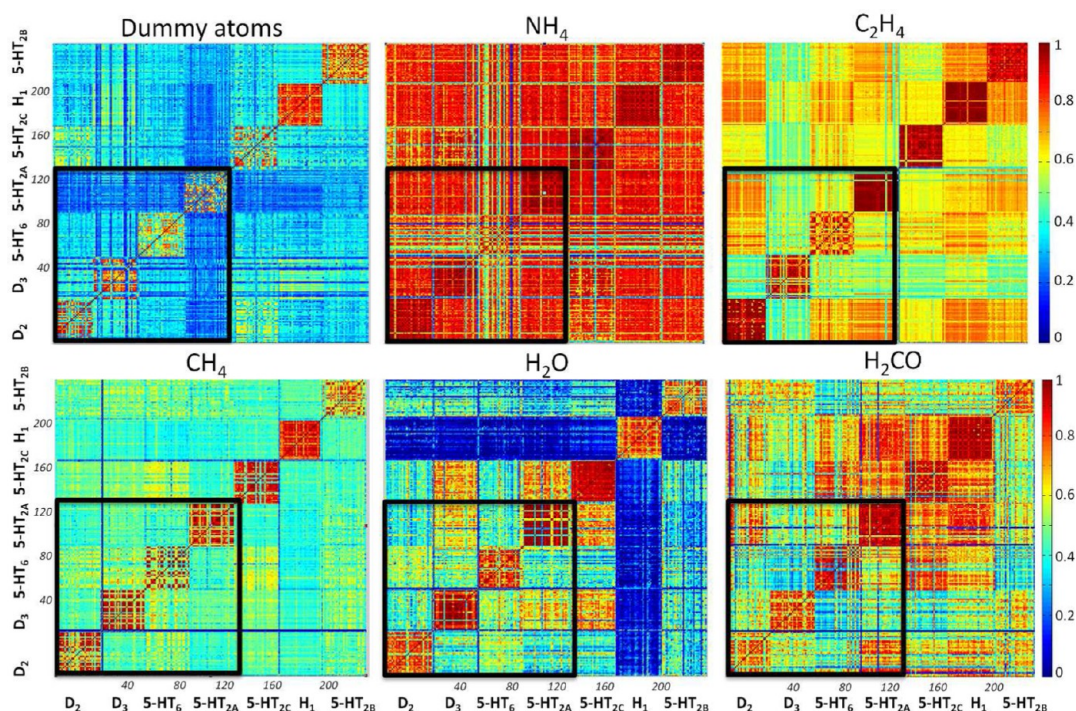


**Figure 3.** Tanimoto coefficient matrices for the molecular probe maps built based on 30 selected conformations of the bioaminergic receptors. The black rectangle separates the matrix of the bioaminergic receptors with a cognition-enhancing effect (group 1) from the bioaminergic receptors causing the side effects (group 2).

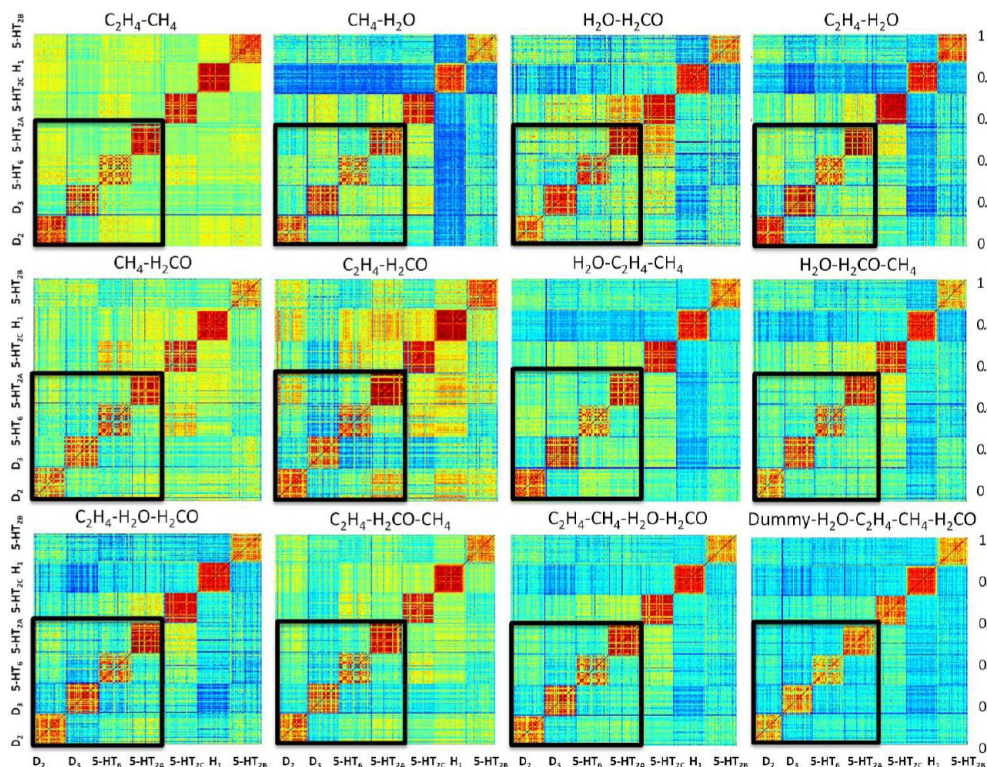


**Figure 4.** Tanimoto coefficient matrices for the combined molecular probe maps built based on 30 selected conformations of the bioaminergic receptors. The black rectangle separates the matrix of the bioaminergic receptors with a cognition-enhancing effect (group 1) from the bioaminergic receptors causing side effects (group 2).

HT<sub>2C</sub><sup>2</sup>, and H<sub>1</sub><sup>2</sup> receptors, anticipating communalities in the donor properties between the receptors.

We then built up the combined probe maps to examine whether the combination of the hydrophilic and hydrophobic

properties are capable of identifying the high similarity within group 1 compared to the receptors in group 2. To do so, we summed up the corresponding Tc values of the probe maps for each receptor conformation and used the average Tc to build

the Tc matrices of combined probe maps as shown in Figure 4. The combination of the two probes shows that  $C_2H_4-CH_4$  has a relatively similar Tc value for all receptors,  $CH_4-H_2O$ ,  $H_2O-H_2CO$ , and  $C_2H_4-H_2O$  have higher Tc values for some conformations, shown in brighter and warmer colors, for several receptors of group 1 and the  $5-HT_{2C}^2$  receptor, and  $CH_4-H_2CO$  and  $C_2H_4-H_2CO$  have relatively high Tc for several conformations of the  $5-HT_{2A}^1$ ,  $5-HT_{2C}^2$ , and  $H_1^2$  receptors.

We then combined three, four, and five probes to further examine similarity and difference between groups. As expected, the increase in a number of probes to build the matrix reduces Tc values as shown by dark green and blue colors in Figure 4.

We quantify the visual analysis of the matrix plots by identifying receptor conformations of group 1, which have Tc value less than 0.5 for the all conformations of the receptors in group 2 and, at the same time, Tc of these conformations is more than 0.5 for at least one conformation of each receptor of group 1. The cutoff of 0.5 was chosen as an arbitrary indicator of similar and different conformations. By screening the receptor conformational space (30 representative conformations for each receptor) using this threshold, we hope to identify conformations of group 1, which provide differences between the receptor groups in the best way and can be used to identify unique pharmacophoric sites that are important for binding with the receptors of group 1. Table 2 shows a number of conformations that meet the established cutoff in the Tc matrices built based on the single and multiple probes. The receptor conformations of group 1 identified by Tc from combination of the  $H_2O$ ,  $C_2H_4$ , and  $CH_4$  probes shows the lowest Tc to the all receptor conformations of group 2 and the highest Tc within group 1. Interestingly, these conformations

have been also selected by several single probes and other combinations of the probes. Although, the  $C_2H_4-H_2O$  combination shows brighter colors, meaning higher Tc, in the part of the matrix formed by receptors of group 1 for several conformations, than in the  $H_2O-C_2H_4-CH_4$  plot, none of the conformations for the  $5-HT_{2A}^1$  receptor met the defined threshold. We, therefore, chose the plot based on the combined Tc using the  $H_2O$ ,  $C_2H_4$ , and  $CH_4$  probes to separate group 1 from group 2. The fact that  $H_2O$ ,  $C_2H_4$ , and  $CH_4$  probes provide the best separation indicates that aromatic, hydrophobic, donor, and acceptor properties are important for the search of the selective molecules targeting group 1. Among other combinations of three probes, the  $H_2O-C_2H_4-CH_4$  plot has brighter and warmer colors in the part of the matrix formed by the receptors of group 1 than in the  $H_2O-H_2CO-CH_4$  and  $C_2H_4-H_2O-H_2CO$  plots.

We have also conducted the molecular probe mapping for two other representative conformations of the first 30 populated clusters of the receptor conformations and had similar results with selection of the  $H_2O-C_2H_4-CH_4$  combination capable of separating receptor conformations distinctly.

To conclude, the molecular probe mapping analysis with the Tc similarity measurement has allowed identifying the receptor conformations with the physicochemical properties, which are similar within group 1 and distinct from the conformational space defined by the receptors of group 2.

**Identification of Pharmacophoric Sites from the Molecular Probe Maps of the Tc-Selected Receptor Conformations.** We then compared the maps of the  $H_2O$ ,  $C_2H_4$ , and  $CH_4$  probes between the receptors of group 1 using the selected conformations (based on the highest Tc of  $H_2O-C_2H_4-CH_4$  probe combination) and clustered the probes to identify the pharmacophoric sites characterizing group 1 of the receptors. To verify the presence or absence of the identified pharmacophore sites in the receptors of group 2, we selected conformations of the receptors with the highest Tc value to the conformations of the receptors of group 1 based on combination of  $H_2O$ ,  $C_2H_4$ , and  $CH_4$  probes. The properties of these conformations of group 2 are meant to be the closest to group 1. The interacting amino acid residues in the found pharmacophore sites, the average interaction energy of probes, and a number of probes are summarized in Table 3 for both groups of the receptors. From analysis of Table 3, we determine common, distinct, and partially distinct pharmacophoric sites between the groups of the receptors, whereas the common pharmacophore sites are present in all receptors and the distinct sites are only in group 1. The partially distinct sites exist in at least three receptors of group 1 and one receptor of group 2 in our study.

The identified pharmacophoric sites of the receptors are shown in Figure 5. Using the receptor conformational space, we were able to identify more pharmacophoric sites compared to the implication of single receptor conformations. Thus, all receptors have four common pharmacophore sites (1–3, 6), in which one of the molecular probes is mapped in all receptors with the favorable interaction energy. The common pharmacophore has two aromatic, one donor, and one hydrophobic site providing general molecular interaction capacities of ligands toward the bioaminergic receptors. Site 6 was more clearly seen in the MD conformations than in the initial structures. We noted that the amino acid residues forming these sites are identical and have similar geometry across the receptors.

**Table 2. Number of Receptor Conformations in Group 1 with the Tanimoto Coefficient Lower Than 0.5 to All Receptors of Group 2 and Higher Than 0.5 to All Receptors of Group 1**

probes	Tc is less than 0.5 to all receptors of group 2				Tc is more than 0.5 to all receptors of group 1			
	D <sub>2</sub>	D <sub>3</sub>	5-HT <sub>2A</sub>	5-HT <sub>6</sub>	D <sub>2</sub>	D <sub>3</sub>	5-HT <sub>2A</sub>	5-HT <sub>6</sub>
dummy atoms	10	16	20	21	7	14	10	15
NH <sub>4</sub>	0	0	0	1	0	0	0	1
C <sub>2</sub> H <sub>4</sub>	0	10	2	0	0	2	2	1
CH <sub>4</sub>	23	16	21	0	1	2	23	0
H <sub>2</sub> CO	2	1	0	1	2	0	0	1
H <sub>2</sub> O	12	5	1	6	7	2	0	0
C <sub>2</sub> H <sub>4</sub> -H <sub>2</sub> O	7	2	0	5	2	2	0	3
C <sub>2</sub> H <sub>4</sub> -CH <sub>4</sub>	0	21	19	1	0	4	3	1
CH <sub>4</sub> -H <sub>2</sub> O	24	2	1	6	15	2	0	2
H <sub>2</sub> O-H <sub>2</sub> CO	2	4	0	4	2	0	2	2
C <sub>2</sub> H <sub>4</sub> -H <sub>2</sub> CO	2	1	0	0	2	0	0	0
CH <sub>4</sub> -H <sub>2</sub> CO	3	2	0	2	3	2	0	1
C <sub>2</sub> H <sub>4</sub> -CH <sub>4</sub> -H <sub>2</sub> O	6	2	2	4	4	2	2	3
C <sub>2</sub> H <sub>4</sub> -H <sub>2</sub> CO-CH <sub>4</sub>	5	6	0	1	5	4	0	1
H <sub>2</sub> O-H <sub>2</sub> CO-CH <sub>4</sub>	6	5	1	4	1	2	1	3
C <sub>2</sub> H <sub>4</sub> -H <sub>2</sub> O-H <sub>2</sub> CO	2	1	0	0	1	0	0	0
C <sub>2</sub> H <sub>4</sub> -CH <sub>4</sub> -H <sub>2</sub> O-H <sub>2</sub> CO	11	3	0	3	0	2	0	2
dummy-H <sub>2</sub> O-C <sub>2</sub> H <sub>4</sub> -CH <sub>4</sub> -H <sub>2</sub> CO	0	5	2	1	0	0	0	0



Table 3. Identified Pharmacophoric Sites from Molecular Probe Maps of the Tc-Selected Receptor Conformations

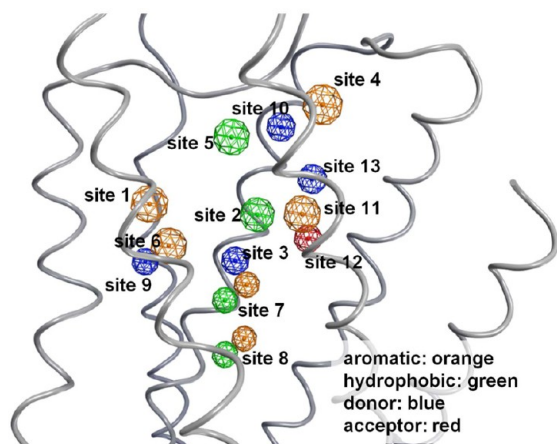
pharmacophore sites	group I						group II				
	Tc-selected conformation (the most different conformation from group 2)						Tc-selected conformation (the most similar conformation to group 1)				
	binding residues	$E_{avr}/N_p(CH_4)$	$E_{avr}/N_p(C_2H_4)$	$E_{avr}/N_p(H_2O)$	binding residues	$E_{avr}/N_p(CH_4)$	$E_{avr}/N_p(C_2H_4)$	$E_{avr}/N_p(H_2O)$			
site 1	S-HT <sub>2A</sub>	F234 <sup>5.47</sup> F339 <sup>6.51</sup> V156 <sup>3.33</sup>	−9/3	−26.7/6	−5.8/3	5-HT <sub>2B</sub>	F226 <sup>5.47</sup> F340 <sup>6.51</sup> V136 <sup>3.33</sup>	−15.2/5	−43.1/10	−8.3/4	
aromatic	S-HT <sub>6</sub>	F197 <sup>5.47</sup> F284 <sup>6.51</sup> V107 <sup>3.33</sup>	−16.1/4	−30.7/8	−6.1/3	S-HT <sub>2C</sub>	F223 <sup>5.47</sup> F327 <sup>6.51</sup> V135 <sup>3.33</sup>	0	−33.6/9	0	
common	D <sub>2</sub>	F198 <sup>5.47</sup> F389 <sup>6.51</sup> V115 <sup>3.33</sup>	−6.2/2	−29/6	−8/4	H <sub>1</sub>	F199 <sup>5.47</sup> Y431 <sup>6.51</sup> Y108 <sup>3.33</sup>	−12.5/4	−32.2/8	−7.1/4	
	D <sub>3</sub>	F197 <sup>5.47</sup> F345 <sup>6.51</sup> V111 <sup>3.33</sup>	−13.8/4	−34.4/9	−4.5/2						
site 2	S-HT <sub>2A</sub>	I152 <sup>3.29</sup> W151 <sup>3.28</sup>	−4.3/2	−2.9/2	−2.9/1	5-HT <sub>2B</sub>	L132 <sup>3.29</sup> W131 <sup>3.28</sup>	−5.6/2	−4.7/1	−10.8/4	
hydrophobic	S-HT <sub>6</sub>	T103 <sup>3.29</sup> W102 <sup>3.28</sup>	−2.2/1	0	−1.6/1	S-HT <sub>2C</sub>	I131 <sup>3.29</sup> W130 <sup>3.28</sup>	−3.4/1	−1.1/1	0	
common	D <sub>2</sub>	V111 <sup>3.29</sup> F110 <sup>3.28</sup>	−4.6/2	−6.5/2	−3.9/2	H <sub>1</sub>	L104 <sup>3.29</sup> W103 <sup>3.28</sup>	−4.5/2	0		
	D <sub>3</sub>	V107 <sup>3.29</sup> F106 <sup>3.28</sup>	−6.5/2	−3.4/2	−2.3/1						
site 3	S-HT <sub>2A</sub>	D155 <sup>3.32</sup>	0	−5.2/2	−34.2/9	5-HT <sub>2B</sub>	D135 <sup>3.32</sup>	0	0	−27.5/14	
donor	S-HT <sub>6</sub>	D106 <sup>3.32</sup>	0	−8.5/2	−28.1/10	S-HT <sub>2C</sub>	D134 <sup>3.32</sup>	0	−3.4/1	−12.2/7	
common	D <sub>2</sub>	D114 <sup>3.32</sup>	0	−5.4/1	−36.45/14	H <sub>1</sub>	D107 <sup>3.32</sup>	0	0	−16.8/8	
	D <sub>3</sub>	D110 <sup>3.32</sup>	0	−14.5/3	−21.1/11						
site 4	S-HT <sub>2A</sub>	W151 <sup>3.28</sup> W141 <sup>EL2</sup>	−10.3/4	−14.7/4	−9.9/5	5-HT <sub>2B</sub>	W131 <sup>3.28</sup> W121 <sup>EL2</sup>	−3.5/1	−7.9/3	0	
aromatic	S-HT <sub>6</sub>	W102 <sup>3.28</sup> W92 <sup>EL2</sup>	0	0	−3.7/2	S-HT <sub>2C</sub>	W130 <sup>3.28</sup> W120 <sup>EL2</sup>	−1.6/1	0	−3/1	
partial	D <sub>2</sub>	F110 <sup>3.28</sup> W100 <sup>EL2</sup>	−11.1/4	−14.2/4	−6.3/3	H <sub>1</sub>	W103 <sup>3.28</sup> W93 <sup>EL2</sup>	0	−1.2/1	0	
	D <sub>3</sub>	F106 <sup>3.28</sup> W96 <sup>EL2</sup>	−10.9/4	−12.1/3	−9.4/5						
site 5	S-HT <sub>2A</sub>	I152 <sup>3.29</sup> L228 <sup>EL2</sup> L229 <sup>EL2</sup>	−9.6/3	−7.3/2	−1.2/1	5-HT <sub>2B</sub>	L132 <sup>3.29</sup> C207 <sup>EL2</sup> V208 <sup>EL2</sup>	−2.3/2	−8.1/2	0	
hydrophobic	S-HT <sub>6</sub>	T103 <sup>3.29</sup> C180 <sup>EL2</sup> R181 <sup>EL2</sup>	0	0	−3.9/2	S-HT <sub>2C</sub>	I131 <sup>3.29</sup> C207 <sup>EL2</sup> V208 <sup>EL2</sup>	−1.1/3	−1.3/1	−1.7/1	
partial	D <sub>2</sub>	V111 <sup>3.29</sup> I184 <sup>EL2</sup> I183 <sup>EL2</sup>	−13.5/5	−5.3/2	−2.7/2	H <sub>1</sub>	L132 <sup>3.29</sup> C207 <sup>EL2</sup> V208 <sup>EL2</sup>	−3.6/1	0	−7.5/5	
	D <sub>3</sub>	V107 <sup>3.29</sup> C181 <sup>EL2</sup> S182 <sup>EL2</sup>	−12.6/3	−1.7/1	−1.7/1						
site 6	S-HT <sub>2A</sub>	F243 <sup>5.47</sup> F340 <sup>6.52</sup> I163 <sup>3.40</sup>	−16.8/5	−37.2/8	−12.8/5	5-HT <sub>2B</sub>	F226 <sup>5.47</sup> F341 <sup>6.52</sup> I143 <sup>3.40</sup>	−12/2	−21.4/3	−7/3	
aromatic	S-HT <sub>6</sub>	F197 <sup>5.47</sup> F285 <sup>6.52</sup> I114 <sup>3.40</sup>	−13.4/3	−23.4/5	−3.3/3	S-HT <sub>2C</sub>	F223 <sup>5.47</sup> F328 <sup>6.52</sup> I142 <sup>3.40</sup>	−11.2/3	−23/4	0	
common	D <sub>2</sub>	F198 <sup>5.47</sup> F350 <sup>6.52</sup> I122 <sup>3.40</sup>	−12.8/4	−27.1/4	0	H <sub>1</sub>	F199 <sup>5.47</sup> F432 <sup>6.52</sup> I115 <sup>3.40</sup>	−14.2/4	−18.8/4	−5.3/2	
	D <sub>3</sub>	F197 <sup>5.47</sup> F346 <sup>6.52</sup> I118 <sup>3.40</sup>	−13.4/3	−19.4/5	−2.4/2						
site 7	S-HT <sub>2A</sub>	L123 <sup>2.53</sup> I163 <sup>3.40</sup> F243 <sup>5.47</sup> W336 <sup>6.48</sup>	−2.7/1	−6.4/2	−2.4/1	5-HT <sub>2B</sub>	V103 <sup>2.53</sup> I143 <sup>3.40</sup> F226 <sup>5.47</sup> W337 <sup>6.48</sup>	−3.9/1	0	0	
hydrophobic	S-HT <sub>6</sub>	V75 <sup>2.53</sup> I114 <sup>3.40</sup> F197 <sup>5.47</sup> W281 <sup>6.48</sup>	−17.5/3	−20.8/4	−2.2/1	S-HT <sub>2C</sub>	V102 <sup>2.53</sup> I142 <sup>3.40</sup> F223 <sup>5.47</sup> W324 <sup>6.48</sup>	0	0	0	
aromatic	D <sub>2</sub>	V83 <sup>2.53</sup> I122 <sup>3.40</sup> F198 <sup>5.47</sup> W386 <sup>6.48</sup>	−12.1/3	−14.4/3	0	H <sub>1</sub>	V80 <sup>2.53</sup> I115 <sup>3.40</sup> F226 <sup>5.47</sup> W428 <sup>6.48</sup>	0	0	−2.7/1	
group 1	D <sub>3</sub>	V78 <sup>2.53</sup> I118 <sup>3.40</sup> F197 <sup>5.47</sup> W342 <sup>6.48</sup>	−5.3/2	−13.2/2	0						
site 8	S-HT <sub>2A</sub>	L123 <sup>2.53</sup> I163 <sup>3.40</sup> F243 <sup>5.47</sup> W336 <sup>6.48</sup>	−3.6/1	−4.7/2	−4.7/2	5-HT <sub>2B</sub>	V103 <sup>2.53</sup> I143 <sup>3.40</sup> F226 <sup>5.47</sup> W337 <sup>6.48</sup>	0	0	0	
hydrophobic	S-HT <sub>6</sub>	V75 <sup>2.53</sup> I114 <sup>3.40</sup> F197 <sup>5.47</sup> W281 <sup>6.48</sup>	−12.8/4	−14.4/3	−2.5/1	S-HT <sub>2C</sub>	V102 <sup>2.53</sup> I142 <sup>3.40</sup> F223 <sup>5.47</sup> W324 <sup>6.48</sup>	0	0	−3.5/2	
aromatic	D <sub>2</sub>	V83 <sup>2.53</sup> I122 <sup>3.40</sup> F198 <sup>5.47</sup> W386 <sup>6.48</sup>	−10.3/3	−5.1/1	0	H <sub>1</sub>	V80 <sup>2.53</sup> I115 <sup>3.40</sup> F226 <sup>5.47</sup> W428 <sup>6.48</sup>	0	−1.7/1	−6.5/3	
group 1	D <sub>3</sub>	V78 <sup>2.53</sup> I118 <sup>3.40</sup> F197 <sup>5.47</sup> W342 <sup>6.48</sup>	−4.1/1	−7.9/3	−0.4/2						
site 9	S-HT <sub>2A</sub>	S239 <sup>5.43</sup> S242 <sup>5.46</sup>	−6/2	−4.5/1	−5.5/2	5-HT <sub>2B</sub>	S222 <sup>5.43</sup> A225 <sup>5.46</sup>	0	0	−2.3/1	
donor	S-HT <sub>6</sub>	S193 <sup>5.43</sup> T196 <sup>5.46</sup>	0	−4.5/1	−5.8/2	S-HT <sub>2C</sub>	S219 <sup>5.43</sup> A222 <sup>5.46</sup>	0	0	0	
group 1	D <sub>2</sub>	S194 <sup>5.43</sup> S197 <sup>5.46</sup>	0	0	−6.2/3	H <sub>1</sub>	A195 <sup>5.43</sup> N198 <sup>5.46</sup>	0	0	0	
	D <sub>3</sub>	S193 <sup>5.43</sup> S196 <sup>5.46</sup>	0	0	−4.2/2						



Table 3. continued

		group I				group II				
		Tc-selected conformation (the most different conformation from group 2)				Tc-selected conformation (the most similar conformation to group 1)				
pharmacophore sites		binding residues	$E_{avr}/N_p(\text{CH}_4)$	$E_{avr}/N_p(\text{C}_2\text{H}_4)$	$E_{avr}/N_p(\text{H}_2\text{O})$		binding residues	$E_{avr}/N_p(\text{CH}_4)$	$E_{avr}/N_p(\text{C}_2\text{H}_4)$	$E_{avr}/N_p(\text{H}_2\text{O})$
site 10	5-HT <sub>2A</sub>	C227 <sup>EL2</sup> W151 <sup>3.28</sup>	−6/2	−1.6/1	−9.6/5	5-HT <sub>2B</sub>	C207 <sup>EL2</sup> W131 <sup>3.28</sup>	−3.9/3	−2.3/2	0
donor	5-HT <sub>6</sub>	C180 <sup>EL2</sup> W102 <sup>3.28</sup>	0	0	−2.2/1	5-HT <sub>2C</sub>	C207 <sup>EL2</sup> W130 <sup>3.28</sup>	−2.4/2	−5.1/4	0
group1	D <sub>2</sub>	C182 <sup>EL2</sup> F110 <sup>3.28</sup>	−4.2/2	−1.8/1	−6.5/3	H <sub>1</sub>	C180 <sup>EL2</sup> W103 <sup>3.28</sup>	−1.7/1	−1.8/2	0
	D <sub>3</sub>	C181 <sup>EL2</sup> F106 <sup>3.28</sup>	−1.6/1	−1.6/1	−5.9/2					
site 11	5-HT <sub>2A</sub>	W151 <sup>3.28</sup> Y370 <sup>7.43</sup>	−4.8/2	−4/1	−2.8/1	5-HT <sub>2B</sub>	W131 <sup>3.28</sup> Y370 <sup>7.43</sup>	−4.6/2	−1.2/1	−3.5/2
aromatic	5-HT <sub>6</sub>	W102 <sup>3.28</sup> Y310 <sup>7.43</sup>	0	−5.2/2	0	5-HT <sub>2C</sub>	W130 <sup>3.28</sup> Y358 <sup>7.43</sup>	−5.4/2	0	−7.1/4
group 1	D <sub>2</sub>	F110 <sup>3.28</sup> Y416 <sup>7.43</sup>	−4.8/2	−11/3	−3.2/2	H <sub>1</sub>	W103 <sup>3.28</sup> Y458 <sup>7.43</sup>	0	0	0
	D <sub>3</sub>	F106 <sup>3.28</sup> Y373 <sup>7.43</sup>	−2.9/1	−13/3	−5.7/3					
site 12	5-HT <sub>2A</sub>	V366 <sup>7.39</sup>	−4.8/2	−4/1	0	5-HT <sub>2B</sub>	V366 <sup>7.39</sup>	−2.6/1	−4.2/1	−2.2/1
acceptor	5-HT <sub>6</sub>	T306 <sup>7.39</sup>	0	0	−5.2/2	5-HT <sub>2C</sub>	V354 <sup>7.39</sup>	−5.4/2	0	0
partial	D <sub>2</sub>	T412 <sup>7.39</sup>	0	−3.7/2	−6.2/3	H <sub>1</sub>	I454 <sup>7.39</sup>	0	0	0
	D <sub>3</sub>	T369 <sup>7.39</sup>	0	−2.2/1	−6.7/3					
site 13	5-HT <sub>2A</sub>	S131 <sup>2.61</sup> Y370 <sup>7.43</sup>	−1.8/1	−3.8/1	0	5-HT <sub>2B</sub>	A111 <sup>2.61</sup> Y370 <sup>7.43</sup>	−9.7/3	−2.9/1	−2.8/2
donor	5-HT <sub>6</sub>	A83 <sup>2.61</sup> Y310 <sup>7.43</sup>	0	0	−4.3/2	5-HT <sub>2C</sub>	S110 <sup>2.61</sup> Y358 <sup>7.43</sup>	−2.5/1	−6.2/2	0
partial	D <sub>2</sub>	V91 <sup>2.61</sup> Y416 <sup>7.43</sup>	−3.4/1	0	−4.1/2	H <sub>1</sub>	N84 <sup>2.61</sup> Y458 <sup>7.43</sup>	0	0	0
	D <sub>3</sub>	V86 <sup>2.61</sup> Y373 <sup>7.43</sup>	−2.5/2	−2.9/2	−5.3/3					

<sup>a</sup> $E_{avr}$  is the average interaction energy between the docked probes and the binding pocket in kilocalories per mole;  $N_p$  is number of the probes docked in the pocket.



**Figure 5.** Identified pharmacophoric sites from molecular probe mapping of the Tc-selected conformations.

Importantly, we have identified five sites that are characteristic for the receptors of group 1 (Figure 5). These are two sites with aromatic and hydrophobic properties (7 and 8, each site is shown in two spheres), two donor (9 and 10), and one aromatic (11) site. The amino acid composition of the pharmacophoric sites is shown in Table 3.

Sites 7 and 8 are formed by residues at positions 2.53, 3.40, 5.47, and 6.48 (the Ballesteros–Weinstein nomenclature,<sup>44</sup> where the most conserved residue in a given helix, X, is assigned the index X.50 and the other residues of the helix are numbered relatively to the 50 position), which are conserved, except the residue at position 2.53. We propose that overall receptor flexibility caused by nonconservative residues localized

in distant sites of the receptors affects the geometry of these conservative residues making the residues prone to form the hydrophobic or aromatic sites at the receptors of group 1. These binding regions have been proposed to interact with the N-propyl group of pramipexole and used to design the pramipexole derivatives with large N-aliphatic or aromatic groups to increase selectivity toward the D<sub>3</sub><sup>1</sup> receptor.<sup>45</sup>

Site 9 is formed by the OH-containing amino acid residues (Ser or Thr) at positions 5.43 and 5.46 in the receptors of group 1, whereas one of these residues in group 2 is Ala (Table 3). The oxygen atom of the OH group of the residue at position 5.46 is exposed to the binding site, suggesting that the ligand with the donor property likely has a good fit in the region. This is because, the hydrogen of the OH group forms a hydrogen bond with the hydrophilic residue at position 3.37. Notably, this hydrogen bond is present in the selected conformations and retains in 40% of the simulation trajectory. Although, the H<sub>1</sub><sup>2</sup> receptor has Asn at position 5.46, Asn does not provide the acceptor region as the carbonyl group interacts with Trp at position 4.57 moving the oxygen atom outside of the binding site. From the mutagenesis studies, it has been suggested that the residue at position 5.46 can be important for ligand selectivity to the 5-HT<sub>6</sub> receptor.<sup>46</sup>

Site 10 involves residues at positions 3.28 and C227<sup>EL2</sup>, which provide the preference to form interactions with the donor group of the ligand through the carbonyl group of C227<sup>EL2</sup>. Although, these residues are conserved, we observed differences in geometry of these residues, especially, in the aromatic residue at position 3.28. The contribution of the second extracellular loop in ligand specificity and the residue at position 3.28 has been suggested for the D<sub>2</sub><sup>1</sup> and D<sub>3</sub><sup>1</sup> receptors.<sup>47,48</sup> The residue swap of F110<sup>3.28</sup> in the D<sub>2</sub><sup>1</sup> receptor

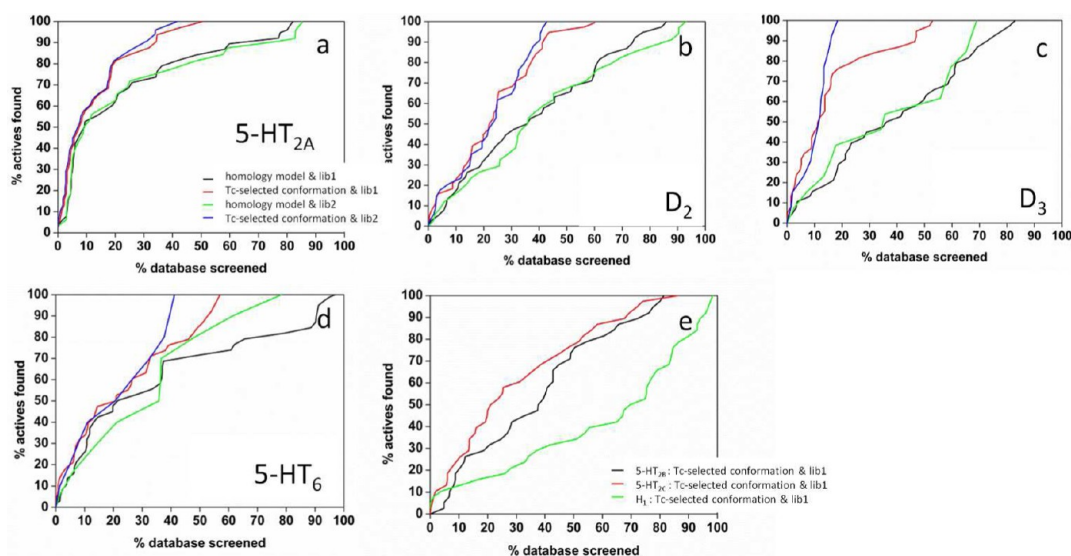


**Figure 6.** Enrichment curves of the retrospective screenings against the Tc-selected MD conformations of the receptors of group 1, the initial conformations of the receptors of group 1 (a–d), and the conformations of the receptors of group 2 that are the most similar to the receptors of group 1 (e).

to W151<sup>3,28</sup> of the 5-HT<sub>2A</sub> receptor and conversely results in the swap of preference toward the binding of dopamine and serotonin.<sup>49</sup>

Site 11 is established by the aromatic residues at positions 3.28 and 7.43. The importance of these residues for selectivity to the D<sub>2</sub><sup>1</sup> receptor has been shown in the mutagenesis studies.<sup>47,50</sup>

In addition, we have identified four partially distinct sites for the receptors of group 1, i.e. aromatic (4), hydrophobic (5), acceptor (12), and donor (13) sites (Figure 5). Thus, partial aromatic and hydrophobic sites (4 and 5) are present in the 5-HT<sub>2A</sub><sup>1</sup>, D<sub>2</sub><sup>1</sup>, and D<sub>3</sub><sup>1</sup> receptors of group 1 and the 5-HT<sub>2B</sub><sup>2</sup> receptor of group 2 (Table 3) as they are found in the initial structures. The acceptor site (12) is in the D<sub>2</sub><sup>1</sup>, D<sub>3</sub><sup>1</sup>, and 5-HT<sub>6</sub><sup>1</sup> receptors of group 1 and the 5-HT<sub>2B</sub><sup>2</sup> receptor of group 2. The donor site (13) is in the 5-HT<sub>6</sub><sup>1</sup>, D<sub>2</sub><sup>1</sup>, and D<sub>3</sub><sup>1</sup> receptors of group 1 and the 5-HT<sub>2B</sub><sup>2</sup> receptor of group 2.

Structurally, site 4 is composed by the aromatic residues at position 3.28 and W141<sup>EL2</sup> in the second extracellular loop, site 5 is formed by the residues at position 3.29, L228<sup>EL2</sup> and L229<sup>EL2</sup>, site 12 is shaped by the residues at positions 7.39 and 7.43 and finally, site 13 is generated by residues at positions 2.61 and 7.43. Sites 12 and 13 can be explained by differences in the hydrogen bond network formed by the nonconservative residues. Thus, Thr at position 7.39 provides the acceptor property in the 5-HT<sub>6</sub><sup>1</sup>, D<sub>2</sub><sup>1</sup>, and D<sub>3</sub><sup>1</sup> receptors, whereas Tyr at position 7.43 provides the donor properties. Note, Tyr at position 7.43 forms a hydrogen bond with the hydrophilic residue at position 2.61 in the 5-HT<sub>2A</sub><sup>1</sup>, 5-HT<sub>2C</sub><sup>2</sup>, and H<sub>1</sub><sup>2</sup> receptors, preventing Tyr from being a donor.

The available mutagenesis and structure–activity relationships studies in the literature suggest the importance of several residues, identified above, in the ligand selectivity to the bioaminergic receptors. Thus, the importance of the residues at positions 2.61, 3.28, and 3.29 for selectivity the D<sub>2</sub><sup>1</sup> receptor has been proposed in two mutagenesis studies.<sup>50,51</sup> The preference of the hydrophilic group or linker such as carboxamide, in the selective compounds to the D<sub>2</sub><sup>1</sup> and D<sub>3</sub><sup>1</sup> receptors<sup>48,52</sup> and the sulfonyl linker in the selective compounds to the 5-HT<sub>6</sub><sup>1</sup> receptor,<sup>53</sup> which are expected to

interact with the region involving helices 2 and 7, has been shown in the structure–activity relationship studies.

Some of the identified pharmacophoric sites in the selected receptor conformations are likely due to long distance effects of the nonconservative residues that provide different shape and physicochemical properties of the binding cavity conservative residues. Indeed, the Difference Evolutionary Trace method and residue-swapping mutagenesis of the predicted residues by this method for the D<sub>2</sub><sup>1</sup> and 5-HT<sub>2A</sub><sup>1</sup> receptors have identified several residues outside of the ligand binding cavity that can affect the affinity of the neurotransmitters, dopamine, and serotonin, by swapping their preference in binding to the receptors. In particular, the swapping of the residues at positions I48<sup>1,48</sup>, M117<sup>3,35</sup>, N124<sup>3,42</sup>, and T205<sup>5,54</sup> in these two receptors changes the selectivity of dopamine and serotonin.<sup>49</sup> Our findings are in line with this experimental study.

Notably, the conformations that enable the capture of the unique features of group 1 are from the clusters of D<sub>3</sub><sup>1</sup>, D<sub>2</sub><sup>1</sup>, 5-HT<sub>6</sub><sup>1</sup>, and 5-HT<sub>2A</sub><sup>1</sup> conformations that contribute to 6%, 4%, 7%, and 10% of simulation trajectory, respectively, and are present in three trajectories obtained from the random velocities.

Our results show that the conformations selected from the MD simulations using molecular probe mapping and the volume-based Tc similarity coefficient, enable the discovery of the pharmacophoric features that are unique for the receptors of group 1, whereas the single receptor crystal structure or homology model failed in identification of these sites and, thus, separation of two receptor groups. These found sites as being useful for selectivity are in correlation with available mutagenesis and structure–activity relationships.

**Retrospective Screening Using the Identified “Selectivity” Receptor Conformations.** We further validated the identified selectivity conformations in the retrospective screening of the available ligands for the receptors of group 1. Thus, the selected conformations of group 1 were used to compare their performance in the retrieval of the known ligands from the random decoy with the initial structures (the crystal structures and homology models) of the receptors as well as with the conformations of the receptors in group 2 with the highest Tc

to group 1. For this purpose, we have collected the set of ligands (Table 3S of the Supporting Information) that bind to the investigated receptors with some preference toward the receptors of group 1 (library 1) and the set of the ligands that bind to one of the receptor of group 1 from the literature sources (library 2). Since not many purely selective ligands to group 1 are available, we have compiled the library of the selective ligands for each receptor of group 1 to examine the docking performance of these molecules against the corresponding receptor (Table 3S of the Supporting Information).

The collected ligands were merged with the diverse library of 500 random compounds (see Methods) and docked to the selected conformations. To validate the performance of the docking procedure we have calculated the enrichment curves, which show the percentage of retrieved active compounds relative to the percentage of the screened library (Figure 6). Overall, in all four receptors the selected conformations of group 1 perform better than the initial conformations of these receptors for both libraries. The enrichment factor for the first 1% and 10% of the screened compound libraries, which are usually used for experimental test, is high in all screenings against selected conformations of group 1 (Table 4S of the Supporting Information). Importantly, the conformations of group 2 that are closer to group 1 have substantially poor performance.

The docked pose for one characteristic ligand, haloperidol, which is selective to group 1, except the 5-HT<sub>6</sub> receptor, in the receptors of group 1 is shown in Figure 7. Thus, in addition to

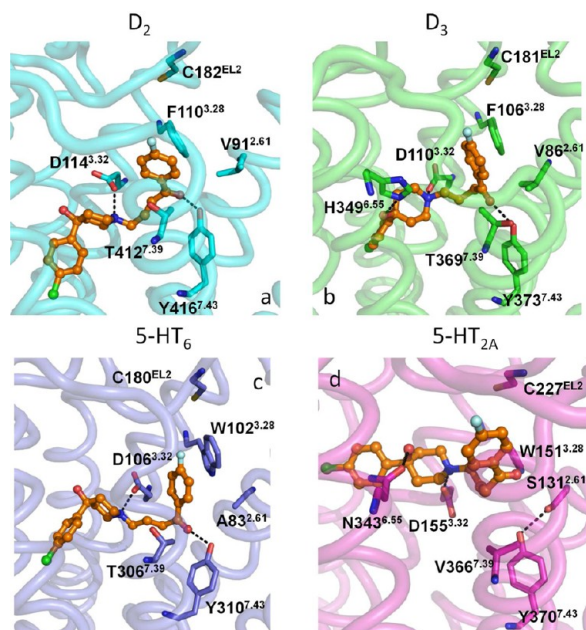


**Figure 7.** Binding pose of haloperidol in the Tc-selected receptor conformations of group 1.

the characteristic interaction with Asp at 3.32 the ligand forms the interactions with the specific sites, i.e. sites 11 and 4 formed by the residues at position 3.28 and site 13 shaped by Tyr at position 7.43, which are identified in the Tc-selected receptor conformations.

Our results suggest that the Tc-selected conformations of the MD simulations can be probed to design selective ligands targeting only the bioaminergic receptors with antipsychotic activity (group 1).

## DISCUSSION

In this work we have proposed a computational structure-based protocol, as flowcharted in Figure 8, which involves the analysis

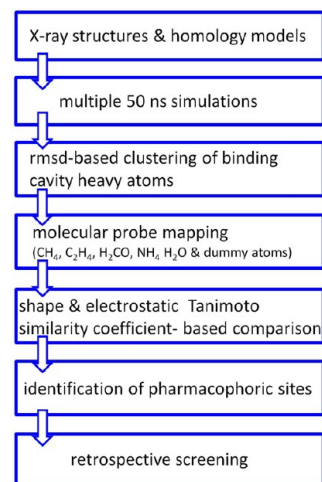


**Figure 8.** Proposed scheme of our computational structure-based protocol in the search of drugs with selective polypharmacology.

of receptor flexibility in the binding cavities across the protein family to tackle ligand selective polypharmacology. As an example, we focus on the bioaminergic receptors family, where several members of the family are targets for psychiatric diseases and others cause unintended side effects. We question whether it is possible to group some dynamic geometrical and physicochemical properties of the ligand binding cavities of the disease-related receptors (group 1), resulting from receptor motions and use these unique properties for the search of drugs targeting this receptor network. The crystal structures of some of the bioaminergic receptors became available in the past few years but implication of structural knowledge to understand polypharmacology of antipsychotic drugs is possible only now.

We first confirm that the three-dimensional coordinates of the receptor binding cavities using a single crystallographic structure or homology model does not allow splitting the receptors in two groups as shown by the derived pharmacophoric sites in Figure 1B. Multiple molecular dynamics simulations of the seven ligand-free receptors were then used to study receptor flexibility and generate conformational ensembles of the receptors. Protein breathing is the basis of protein recognition and function, and therefore, consideration of multiple conformations of proteins can reveal the dynamic properties necessary for receptor physiological and pathological responses. The measurements of the volume and solvent accessible surface area of the receptor binding cavities suggest notable flexibility of side chains and likely appearance of novel binding regions. The rmsd-based clustering of the heavy atoms of the binding cavities shows a different degree of structural diversity in the receptors and stimulates further investigations of the receptor conformational space. From clustering of the MD simulation trajectories, we removed redundant and selected the most diverse and dominant conformations of the receptors for comparison of their binding properties.

In order to navigate across the selected conformational space of all receptors and enable comparison of the receptor properties regardless of residue differences, we unify the conformational space of the receptors via molecular probe



mapping. A probe mapping technique, where low-molecular weight molecules or fragments, so-called probes, are docked to the active site to identify specific binding regions, was formulated almost four decades ago<sup>54</sup> and since then has been largely explored<sup>55–59</sup> and successfully used to design novel ligands.<sup>11,60–62</sup> The implication of molecular probe mapping together with MD simulations in structure-based drug design has been first developed in building a dynamic pharmacophore for binding to HIV-1 integrase by Carlson et al.<sup>7</sup> Here, we apply probe mapping in combination with MD simulations to address ligand selective polypharmacology. In our work, we translate residue three-dimensional information and its property to a favorable position of a specific type probe in the binding cavities of the receptors. As result, we describe the binding cavity of the receptors in the form of three-dimensional probe maps and apply this description to the selected ensemble of the receptor conformations of all receptors. The generated multiple probe maps of the receptors can be then compared based on the geometrical and physicochemical properties using a simple technique.

All-against-all comparison of the probe maps was conducted using the shape-based or electrostatic Tanimoto similarity coefficient.<sup>22</sup> We chose Tc similarity measurement due to its simplicity and availability of the software package for its calculation. Tanimoto similarity enabled us to compare the individual and combination of probe maps, thus providing comparison of various properties of the binding regions in the cavity simultaneously.

By comparison of the probe maps, we were able to identify receptor conformations of group 1 that have distinct properties from the receptors of group 2 defined by the Tc cutoff of 0.5. The selected cutoff was chosen arbitrarily and more tests should be carried out to understand the chemical sense of the choice. We nevertheless use the conformations of the receptors selected by Tc equal to 0.5, i.e. the conformations of the receptors of group 1 with the lowest Tc value to all receptors of group 2 and the conformations of the receptors of group 2 with the highest Tc value to all receptors of group 1 to visualize potential regions of differences and similarities between groups of the receptors. To perform this task, we built a pharmacophore based on the probe maps of the Tc-selected conformations. The developed pharmacophore has common, distinct, and partially distinct sites between the groups of the receptors. Importantly, we found the pharmacophoric sites that are unique for the receptors of group 1, thus identified residues that might be important for ligand selective binding. In particular, we predicted that residues at positions 2.53, 3.40, 5.47, 6.48, 5.43, 5.46, 3.28, and C227<sup>EL2</sup> are likely of importance in development of effective antipsychotic drugs with the reduced off-target activities. The impact of some of these residues to ligand selectivity has been suggested from residue mutagenesis and ligand structure–activity relationships studies.<sup>45–53</sup>

To further examine the Tc-selected conformations of the receptors, we conducted the retrospective screenings of the libraries containing the known ligands with some preference of binding to the receptors of group 1. We identified better performance for the selected conformations of group 1 in retrieval of the known ligands than the most similar conformations of group 2. However, we admit that only predictive screening can provide information on potential implication of the identified receptor conformations for the search of ligands having selective polypharmacology.

Polypharmacology of drugs has been tackled computationally via comparison of the binding sites and ligand–protein interactions using available crystal structures of the ligand–protein complexes in a number of studies.<sup>63–68</sup> Various approaches in coding of protein and ligand atoms as well as similarity search algorithms have been utilized to compare proteins in these studies. Here, we propose a computational structure-based protocol that uses molecular dynamics simulations, molecular probe mapping, and Tanimoto similarity measurement to address the selective polypharmacology of antipsychotic drugs targeting the bioaminergic receptors. Our study shows that by understanding differences in the binding cavity through its flexibility, we can identify residues that affect the ability to bind the ligand and also suggest the part of the ligand that might be modified to achieve selective binding. The combination of techniques, we use here, represents an efficient method to identify unique properties of the disease-related proteins on the reduced diverse conformational space and provides a novel application of existing computational methods for the investigation of structural reasons of selective polypharmacology. The protocol is particularly relevant in the cases when selective ligands targeting a set of proteins are not available and the unliganded protein structures can sample the liganded form of the protein in the MD simulations. Another advantage of the proposed protocol is the use of the readily available software packages.

## ■ ASSOCIATED CONTENT

### § Supporting Information

Figure of the receptor sequence alignment, table of the ligand binding cavity properties in the bioaminergic receptors, table of the pharmacophoric sites derived from the MD initial structures, the library of the antipsychotic drugs, and table of enrichment factors. This material is available free of charge via the Internet at <http://pubs.acs.org>.

## ■ AUTHOR INFORMATION

### Corresponding Author

\*Telephone: +44 289 097 2202. Fax: +44 289 024 7794. E-mail: [i.tikhonova@qub.ac.uk](mailto:i.tikhonova@qub.ac.uk).

### Notes

The authors declare no competing financial interest.

## ■ ACKNOWLEDGMENTS

We thank Dr. John King for a generous donation to establish a medicinal chemistry laboratory at the School of Pharmacy of Queen's University Belfast and for providing a Ph.D. studentship for B.S. S.L.P. thanks Wellcome Trust Biomedical Vacation Scholarship. The research in the group of I.G.T. is supported by the Royal Society (RG2010/R2). We used the high-performance computational facilities of Queen's University Belfast. We thank Dr. Charles Longhton for helpful discussions.

## ■ REFERENCES

- (1) Hopkins, A. L. Network pharmacology. *Nat. Biotechnol.* **2007**, *10*, 1110–1111.
- (2) Allen, J. A.; Roth, B. L. Strategies to discover unexpected targets for drugs active at G protein-coupled receptors. *Ann. Rev. Pharmacol. Toxicol.* **2011**, *51*, 117–144.
- (3) Roth, B. L.; Sheffler, D. J.; Kroeze, W. K. Magic shotguns versus magic bullets: selectively non-selective drugs for mood disorders and schizophrenia. *Nat. Rev. Drug Discov.* **2004**, *4*, 353–359.

- (4) Cavalli, A.; Bolognesi, M. L. Neglected tropical diseases: multi-target-directed ligands in the search for novel lead candidates against *Trypanosoma* and *Leishmania*. *J. Med. Chem.* **2009**, *23*, 7339–7359.
- (5) Ivetac, A.; McCammon, J. A. Mapping the druggable allosteric space of G-protein coupled receptors: a fragment-based molecular dynamics approach. *Chem. Biol. Drug Des.* **2010**, *3*, 201–217.
- (6) Durrant, J. D.; McCammon, J. A. Molecular dynamics simulations and drug discovery. *BMC Biol.* **2011**, *71*.
- (7) Carlson, H. A.; Masukawa, K. M.; Rubins, K.; Bushman, F. D.; Jorgensen, W. L.; Lins, R. D.; Briggs, J. M.; McCammon, J. A. Developing a dynamic pharmacophore model for HIV-1 integrase. *J. Med. Chem.* **2000**, *11*, 2100–2114.
- (8) Amaro, R. E.; Schnaufer, A.; Interthal, H.; Hol, W.; Stuart, K. D.; McCammon, J. A. Discovery of drug-like inhibitors of an essential RNA-editing ligase in *Trypanosoma brucei*. *Proc. Natl. Acad. Sci. U.S.A.* **2008**, *45*, 17278–17283.
- (9) Durrant, J. D.; Urbaniak, M. D.; Ferguson, M. A.; McCammon, J. A. Computer-aided identification of *Trypanosoma brucei* uridine diphosphate galactose 4'-epimerase inhibitors: toward the development of novel therapies for African sleeping sickness. *J. Med. Chem.* **2010**, *13*, S025–S032.
- (10) Cheng, L. S.; Amaro, R. E.; Xu, D.; Li, W. W.; Arzberger, P. W.; McCammon, J. A. Ensemble-based virtual screening reveals potential novel antiviral compounds for avian influenza neuraminidase. *J. Med. Chem.* **2008**, *13*, 3878–3894.
- (11) Bowman, A. L.; Nikolovska-Coleska, Z.; Zhong, H.; Wang, S.; Carlson, H. A. Small molecule inhibitors of the MDM2-p53 interaction discovered by ensemble-based receptor models. *J. Am. Chem. Soc.* **2007**, *42*, 12809–12814.
- (12) Pentikainen, U.; Settimo, L.; Johnson, M. S.; Pentikainen, O. T. Subtype selectivity and flexibility of ionotropic glutamate receptors upon antagonist ligand binding. *Org. Biomol. Chem.* **2006**, *6*, 1058–1070.
- (13) Zeng, J.; Li, W.; Zhao, Y.; Liu, G.; Tang, Y.; Jiang, H. Insights into ligand selectivity in estrogen receptor isoforms: Molecular dynamics simulations and binding free energy calculations. *J. Phys. Chem. B* **2008**, *9*, 2719–2726.
- (14) Martinez, L.; Nascimento, A. S.; Nunes, F. M.; Phillips, K.; Aparicio, R.; Dias, S. M. G.; Figueira, A. C. M.; Lin, J. H.; Nguyen, P.; Apriletti, J. W.; Neves, F. A. R.; Baxter, J. D.; Webb, P.; Skaf, M. S.; Polikarpov, I. Gaining ligand selectivity in thyroid hormone receptors via entropy. *Proc. Natl. Acad. Sci. U.S.A.* **2009**, *49*, 20717–20722.
- (15) Babakhani, A.; Talley, T. T.; Taylor, P.; McCammon, J. A. A virtual screening study of the acetylcholine binding protein using a relaxed-complex approach. *Comput. Biol. Chem.* **2009**, *2*, 160–170.
- (16) Selvam, B.; Wereszczynski, J.; Tikhonova, I. G. Comparison of Dynamics of Extracellular Accesses to the beta(1) and beta(2) Adrenoceptors Binding Sites Uncovers the Potential of Kinetic Basis of Antagonist Selectivity. *Chem. Biol. Drug Des.* **2012**, *2*, 215–226.
- (17) Bowman, A. L.; Lerner, M. G.; Carlson, H. A. Protein flexibility and species specificity in structure-based drug discovery: Dihydrofolate reductase as a test system. *J. Am. Chem. Soc.* **2007**, *12*, 3634–3640.
- (18) Ferrari, S.; Costi, P. M.; Wade, R. C. Inhibitor specificity via protein dynamics: insights from the design of antibacterial agents targeted against thymidylate synthase. *Chem. Biol.* **2003**, *12*, 1183–1193.
- (19) Xie, L.; Evangelidis, T.; Xie, L.; Bourne, P. E. Drug discovery using chemical systems biology: weak inhibition of multiple kinases may contribute to the anti-cancer effect of nelfinavir. *PLoS Comput. Biol.* **2011**, *4*, e1002037.
- (20) Chien, E. Y.; Liu, W.; Zhao, Q.; Katritch, V.; Han, G. W.; Hanson, M. A.; Shi, L.; Newman, A. H.; Javitch, J. A.; Cherezov, V.; Stevens, R. C. Structure of the human dopamine D3 receptor in complex with a D2/D3 selective antagonist. *Science* **2010**, *6007*, 1091–1095.
- (21) Shimamura, T.; Shiroishi, M.; Weyand, S.; Tsujimoto, H.; Winter, G.; Katritch, V.; Abagyan, R.; Cherezov, V.; Liu, W.; Han, G. W.; Kobayashi, T.; Stevens, R. C.; Iwata, S. Structure of the human histamine H1 receptor complex with doxepin. *Nature* **2011**, *7354*, 65–70.
- (22) ROCS 3.1.2 and EON 2.1.0; OpenEye Scientific Software, Inc.: Santa Fe, NM, 2010.
- (23) Prime 2.2; Schrödinger, LLC: New York, NY, 2008.
- (24) Schrodinger suite 9.0; Schrodinger, LLC: New York, NY, 2010.
- (25) MacKerell, A.; Bashford, D.; Bellott, M.; Dunbrack, R.; Evanseck, J.; Field, M.; Fischer, S.; Gao, J.; Guo, H.; Ha, S.; Joseph-McCarthy, D.; Kuchnir, L.; Kucsera, K.; Lau, F.; Mattos, C.; Michnick, S.; Ngo, T.; Nguyen, D.; Prodhom, B.; Reiher, W.; Roux, B.; Schlenkrich, M.; Smith, J.; Stote, R.; Straub, J.; Watanabe, M.; Wiorkiewicz-Kuczera, J.; Yin, D.; Karplus, M. All-atom empirical potential for molecular modeling and dynamics studies of proteins. *J. Phys. Chem. B* **1998**, *18*, 3586–3616.
- (26) Laskowski, R. A.; Macarthur, M. W.; Moss, D. S.; Thornton, J. M. Procheck - a Program to Check the Stereochemical Quality of Protein Structures. *J. Appl. Crystallogr.* **1993**, *26*, 283–291.
- (27) Bowers, K. J.; Chow, E.; Xu, H.; Dror, R. O.; Eastwood, M. P.; Gregersen, B. A.; Klepeis, J. L.; Kolossváry, I.; Moraes, M. A.; Sacerdoti, F. D.; Salmon, J. K.; Shan, Y.; Shaw D. E. In *Scalable Algorithms for Molecular Dynamics Simulations on Commodity Clusters*; Proceedings of the ACM/IEEE Conference on Supercomputing, Tampa, FL, Nov 11–17, 2006; pp SC06.
- (28) Darden, T.; York, D.; Pedersen, L. Particle Mesh Ewald - an N.Log(n) Method for Ewald Sums in Large Systems. *J. Chem. Phys.* **1993**, *12*, 10089–10092.
- (29) Humphrey, W.; Dalke, A.; Schulten, K. VMD: Visual molecular dynamics. *J. Mol. Graph.* **1996**, *1*, 33–38.
- (30) Durrant, J. D.; de Oliveira, C. A.; McCammon, J. A. POVME: an algorithm for measuring binding-pocket volumes. *J. Mol. Graph. Model.* **2011**, *5*, 773–776.
- (31) Berendsen, H. J. C.; Vanderspoel, D.; Vandrunen, R. Gromacs - a Message-Passing Parallel Molecular-Dynamics Implementation. *Comput. Phys. Commun.* **1995**, *1–3*, 43–56.
- (32) Molecular Operating Environment (MOE); Montreal, Canada, 2013.
- (33) MathWorks MatLab; Matrix House, Cambridge, UK, 2013.
- (34) Glide 5.6; Schrödinger, LLC: New York, NY, 2009.
- (35) Johnson, M.; Antonio, T.; Reith, M. E.; Dutta, A. K. Structure-activity relationship study of N(6)-(2-(4-(1H-Indol-5-yl)piperazin-1-yl)ethyl)-N(6)-propyl-4,5,6,7-tetrahydrobenzo[d]thiazole-2,6-diamine analogues: development of highly selective D3 dopamine receptor agonists along with a highly potent D2/D3 agonist and their pharmacological characterization. *J. Med. Chem.* **2012**, *12*, S826–S840.
- (36) Nelson, D. L.; Lucaites, V. L.; Wainwright, D. B.; Glennon, R. A. Comparisons of hallucinogenic phenylisopropylamine binding affinities at cloned human 5-HT<sub>2A</sub>, -HT<sub>2B</sub> and 5-HT<sub>2C</sub> receptors. *Naunyn-Schmiedeberg's Arch. Pharmacol.* **1999**, *1*, 1–6.
- (37) Luedtke, R. R.; Mishra, Y.; Wang, Q.; Griffin, S. A.; Bell-Horner, C.; Taylor, M.; Vangveravong, S.; Dillon, G. H.; Huang, R. Q.; Reichert, D. E.; Mach, R. H. Comparison of the binding and functional properties of two structurally different D2 dopamine receptor subtype selective compounds. *ACS Chem. Neurosci.* **2012**, *12*, 1050–1062.
- (38) Marti-Renom, M. A.; Stuart, A. C.; Fiser, A.; Sanchez, R.; Melo, F.; Sali, A. Comparative protein structure modeling of genes and genomes. *Annu. Rev. Biophys. Biomol. Struct.* **2000**, *291*–325.
- (39) Wang, C.; Jiang, Y.; Ma, J.; Wu, H.; Wacker, D.; Katritch, V.; Han, G. W.; Liu, W.; Huang, X. P.; Vardy, E.; McCorvy, J. D.; Gao, X.; Zhou, E. X.; Melcher, K.; Zhang, C.; Bai, F.; Yang, H.; Yang, L.; Jiang, H.; Roth, B. L.; Cherezov, V.; Stevens, R. C.; Xu, H. E. Structural Basis for Molecular Recognition at Serotonin Receptors. *Science* **2013**, *6132*, 610–614.
- (40) Huang, J.; Chen, S.; Zhang, J. J.; Huang, X. Y. Crystal structure of oligomeric beta-adrenergic G protein-coupled receptors in ligand-free basal state. *Nat. Struct. Mol. Biol.* **2013**, *4*, 419–425.
- (41) Warne, T.; Serrano-Vega, M. J.; Baker, J. G.; Moukhametzianov, R.; Edwards, P. C.; Henderson, R.; Leslie, A. G.; Tate, C. G.; Schertler, G. F. Structure of a beta1-adrenergic G-protein-coupled receptor. *Nature* **2008**, *7203*, 486–491.

- (42) Rush, T. S., 3rd; Grant, J. A.; Mosyak, L.; Nicholls, A. A shape-based 3-D scaffold hopping method and its application to a bacterial protein-protein interaction. *J. Med. Chem.* **2005**, *5*, 1489–1495.
- (43) Grant, J.; Gallardo, M.; Pickup, B. A fast method of molecular shape comparison: A simple application of a Gaussian description of molecular shape. *J. Comput. Chem.* **1996**, *14*, 1653–1666.
- (44) Ballesteros, J. A.; Weinstein, H. Integrated methods for the construction of three-dimensional models and computational probing of structure-function relations in G protein-coupled receptors. *Methods Neurosci.* **1995**, *366*–428.
- (45) Chen, J.; Collins, G. T.; Zhang, J.; Yang, C. Y.; Levant, B.; Woods, J.; Wang, S. Design, synthesis, and evaluation of potent and selective ligands for the dopamine 3 (D3) receptor with a novel in vivo behavioral profile. *J. Med. Chem.* **2008**, *19*, S905–S908.
- (46) Boess, F. G.; Monsma, F. J., Jr; Meyer, V.; Zwingelstein, C.; Sleight, A. J. Interaction of tryptamine and ergoline compounds with threonine 196 in the ligand binding site of the 5-hydroxytryptamine6 receptor. *Mol. Pharmacol.* **1997**, *3*, 515–523.
- (47) Lan, H.; Durand, C. J.; Teeter, M. M.; Neve, K. A. Structural determinants of pharmacological specificity between D(1) and D(2) dopamine receptors. *Mol. Pharmacol.* **2006**, *1*, 185–194.
- (48) Banala, A. K.; Levy, B. A.; Khatri, S. S.; Furman, C. A.; Roof, R. A.; Mishra, Y.; Griffin, S. A.; Sibley, D. R.; Luedtke, R. R.; Newman, A. H. N-(3-fluoro-4-(4-(2-methoxy or 2,3-dichlorophenyl)piperazine-1-yl)butyl)arylcarboxamides as selective dopamine D3 receptor ligands: critical role of the carboxamide linker for D3 receptor selectivity. *J. Med. Chem.* **2011**, *10*, 3581–3594.
- (49) Rodriguez, G. J.; Yao, R.; Lichtarge, O.; Wensel, T. G. Evolution-guided discovery and recoding of allosteric pathway specificity determinants in psychoactive bioamine receptors. *Proc. Natl. Acad. Sci. U.S.A.* **2010**, *17*, 7787–7792.
- (50) Cummings, D. F.; Ericksen, S. S.; Schetz, J. A. Three amino acids in the D2 dopamine receptor regulate selective ligand function and affinity. *J. Neurochem.* **2009**, *1*, 45–57.
- (51) Simpson, M. M.; Ballesteros, J. A.; Chiappa, V.; Chen, J.; Suehiro, M.; Hartman, D. S.; Godel, T.; Snyder, L. A.; Sakmar, T. P.; Javitch, J. A. Dopamine D4/D2 receptor selectivity is determined by A divergent aromatic microdomain contained within the second, third, and seventh membrane-spanning segments. *Mol. Pharmacol.* **1999**, *6*, 1116–1126.
- (52) Ehrlich, K.; Gotz, A.; Bollinger, S.; Tschammer, N.; Bettinetti, L.; Harterich, S.; Hubner, H.; Lanig, H.; Gmeiner, P. Dopamine D2, D3, and D4 selective phenylpiperazines as molecular probes to explore the origins of subtype specific receptor binding. *J. Med. Chem.* **2009**, *15*, 4923–4935.
- (53) Liu, K. G.; Lo, J. R.; Comery, T. A.; Zhang, G. M.; Zhang, J. Y.; Kowal, D. M.; Smith, D. L.; Di, L.; Kerns, E. H.; Schechter, L. E.; Robichaud, A. J. 1-Sulfonylindazoles as potent and selective 5-HT6 ligands. *Bioorg. Med. Chem. Lett.* **2009**, *9*, 2413–2415.
- (54) Goodford, P. J. A computational procedure for determining energetically favorable binding sites on biologically important macromolecules. *J. Med. Chem.* **1985**, *7*, 849–857.
- (55) Stultz, C. M.; Karplus, M. MCSS functionality maps for a flexible protein. *Proteins* **1999**, *4*, 512–529.
- (56) Mattos, C.; Ringe, D. Locating and characterizing binding sites on proteins. *Nat. Biotechnol.* **1996**, *5*, 595–599.
- (57) Dennis, S.; Kortvelyesi, T.; Vajda, S. Computational mapping identifies the binding sites of organic solvents on proteins. *Proc. Natl. Acad. Sci. U.S.A.* **2002**, *7*, 4290–4295.
- (58) Silberstein, M.; Dennis, S.; Brown, L.; Kortvelyesi, T.; Clodfelter, K.; Vajda, S. Identification of substrate binding sites in enzymes by computational solvent mapping. *J. Mol. Biol.* **2003**, *5*, 1095–1113.
- (59) Kastenholz, M. A.; Pastor, M.; Cruciani, G.; Haaksma, E. E.; Fox, T. GRID/CPGA: a new computational tool to design selective ligands. *J. Med. Chem.* **2000**, *16*, 3033–3044.
- (60) Greer, J.; Erickson, J. W.; Baldwin, J. J.; Varney, M. D. Application of the three-dimensional structures of protein target molecules in structure-based drug design. *J. Med. Chem.* **1994**, *8*, 1035–1054.
- (61) von Itzstein, M.; Dyason, J. C.; Oliver, S. W.; White, H. F.; Wu, W. Y.; Kok, G. B.; Pegg, M. S. A study of the active site of influenza virus sialidase: an approach to the rational design of novel anti-influenza drugs. *J. Med. Chem.* **1996**, *2*, 388–391.
- (62) Brincat, J. P.; Carosati, E.; Sabatini, S.; Manfroni, G.; Fravolini, A.; Raygada, J. L.; Patel, D.; Kaatz, G. W.; Cruciani, G. Discovery of novel inhibitors of the NorA multidrug transporter of *Staphylococcus aureus*. *J. Med. Chem.* **2011**, *1*, 354–365.
- (63) Kinnings, S. L.; Jackson, R. M. Binding site similarity analysis for the functional classification of the protein kinase family. *J. Chem. Inf. Model.* **2009**, *2*, 318–329.
- (64) Tanramluk, D.; Schreyer, A.; Pitt, W. R.; Blundell, T. L. On the origins of enzyme inhibitor selectivity and promiscuity: a case study of protein kinase binding to staurosporine. *Chem. Biol. Drug Des.* **2009**, *1*, 16–24.
- (65) Hoffmann, B.; Zaslavskiy, M.; Vert, J. P.; Stoven, V. A new protein binding pocket similarity measure based on comparison of clouds of atoms in 3D: application to ligand prediction. *BMC Bioinf.* **2010**, *99*–2105–11–99.
- (66) Sciabola, S.; Stanton, R. V.; Mills, J. E.; Flocco, M. M.; Baroni, M.; Cruciani, G.; Perruccio, F.; Mason, J. S. High-throughput virtual screening of proteins using GRID molecular interaction fields. *J. Chem. Inf. Model.* **2010**, *1*, 155–169.
- (67) Milletti, F.; Vulpatti, A. Predicting polypharmacology by binding site similarity: from kinases to the protein universe. *J. Chem. Inf. Model.* **2010**, *8*, 1418–1431.
- (68) Sturm, N.; Desaphy, J.; Quinn, R. J.; Rognan, D.; Kellenberger, E. Structural insights into the molecular basis of the ligand promiscuity. *J. Chem. Inf. Model.* **2012**, *9*, 2410–2421.